energies

MDPI

Article

Breathing Planet Earth: Analysis of Keeling's Data on CO_2 and O_2 with Respiratory Quotient (RQ), Part I: Global Respiratory Quotient (RQ_{Glob}) of Earth

Kalyan Annamalai

J. Mike Walker '66 Department of Mechanical Engineering, Texas A&M University, College Station, TX 77843-3123, USA; kannamalai@tamu.edu

Abstract: In biology, respiratory quotient (*RQ*) is defined as the ratio of CO_2 moles produced per mole of oxygen consumed. Recently, Annamalai et al. applied the *RQ* concept to engineering literature to show that CO_2 emission in Giga Tons per Exa J of energy = $0.1 * RQ$. Hence, the *RQ* is a measure of CO_2 released per unit of energy released during combustion. Power plants on earth use a mix of fossil fuels (FF), and the *RQ* of the mix is estimated as 0.75. Keeling's data on CO_2 and O_2 concentrations in the atmosphere (abbreviated as atm., 1991–2018) are used to determine the average RQ_{Glob} of earth as 0.47, indicating that 0.47 "net" moles of CO_2 are added to which means that there is a net loss of 5.6 kg C(s) from earth per mole of O_2 depleted in the absence of sequestration, or the mass loss rate of earth is estimated at 4.3 GT per year. Based on recent literature on the earth's tilt and the amount of water pumped, it is speculated that there could be an additional tilt of 2.7 cm over the next 17 years. While *RQ* of FF, or biomass, is a property, RQ_{Glob} is not. It is shown that the lower the RQ_{Glob}, the higher the acidity of oceans, the lesser the CO_2 addition to atm, and the lower the earth's mass loss. Keeling's saw-tooth pattern of O_2 is predicted from known CO_2 data and RQ_{Glob}. In Part II, the *RQ* concept is expanded to define energy-based $RQ_{Glob,En}$, and adopt the CO_2 and O_2 balance equations, which are then used in developing the explicit relations for CO_2 distribution amongst atm., land, and ocean, and the *RQ*-based results are validated with results from more detailed literature models for the period 1991–2018.

Keywords: CO_2 budget; global respiratory quotient; fossil energy; biology and planet

Citation: Annamalai, K. Breathing Planet Earth: Analysis of Keeling's Data on CO_2 and O_2 with Respiratory Quotient (RQ), Part I: Global Respiratory Quotient (RQ_{Glob}) of Earth. *Energies* **2024**, *17*, 299. https://doi.org/10.3390/en17020299

Academic Editors: Long Yu, Huanquan Pan and Jinjie Wang

Received: 1 September 2023
Revised: 14 November 2023
Accepted: 22 November 2023
Published: 7 January 2024

1. Introduction

According to Biology Online [1], life is defined as "a distinctive characteristic of a living organism from a dead organism or non-living thing, as specifically distinguished by the capacity to grow, metabolize, respond (to stimuli), adapt, and reproduce". On the other hand, non-biological systems (NBS) include thermal systems (e.g., heat engines, power plants, etc.) which convert the chemical energy of fossil fuels (FF) into work via rapid oxidation or combustion. The NBS "breathe" in oxygen, oxidizes FF, which includes natural gas, oil, and coal, and "breathe" out CO_2 and H_2O. The metabolism of nutrients (or fuels) in many biological systems (including BS, humans, land and ocean animals, plants, etc.) involves slow oxidation, consuming oxygen, and then breathing out CO_2. In biology, the ratio of moles of CO_2 produced to O_2 moles used in the release of energy is called the respiration quotient (*RQ*). Like NBS and BS, the earth undergoes a breathing cycle, but with a difference. While NBS, particularly humans, cannot naturally produce oxygen, terrestrial ecosystems include trees and plants on land, and phytoplankton (PP) in oceans "breathe" in CO_2 and "breathe" out O_2 under photosynthesis (PS), where C is stored as the growth mass of biomass. In addition, biomass undergoes a "respiration" process, which is used to oxidize sugars for life-sustaining functions during the growth of biomass [2,3]. In addition to CO_2 from FF, the dead organic matter releases $CO_2 \approx 50$ GT/year). The net primary product (NPP) of C i during the photosynthesis is the difference between the gross

primary production (GPP, ≈120 GT of C/year and the C used in the respiration process (≈60 GT of C/year) and hence the NPP during photosynthesis is about 60 GT of C/year while decomposition of biomass is about 50 GT/year. Thus, the NEP of the ecosystem is 10 GT/year [4]. It is apparent that biomass serves as a CO_2 sink and an O_2 source in the growth of biomass, (i.e., CO_2 is split into C(s) and O_2). As used here, the term biomass represents both terrestrial and ocean-based plants. For biomass growth, the CO_2 literature uses a photosynthetic quotient (PQ = O_2 mols produced/CO_2 mols used), which is the inverse of *RQ* used in biology and various other terms (more details in Section 3).

In addition, CO_2 is mainly released from the combustion of FF (e.g., coal, oil, gasoline, diesel, kerosene, and natural gas) in power plants, land uses, and industrial processes; the corresponding decrease in O_2 in the atm is due to the consumption of fossil fuels. The CO_2 emissions reached about 36.3 giga tons (GT) of CO_2 in 2021, and a majority (almost 80%) of the total carbon emissions have been due to coal and liquid fuels, with about 20% from the combustion of gaseous fuels [5].

Apart from biomass, which serves as the CO_2 sink, CO_2 is also stored in the ocean. The difference between CO_2 produced and CO_2 sinks via biomass and ocean storage results in the accumulation of CO_2 in the atmosphere $\{d[CO_2]/d\}_{atm}$, and the difference between O_2 consumed for oxidation of FF and O_2 produced by biomass results in the net depletion of O_2 from the atmosphere $\{d[O_2]/dt\}_{atm}$. Since 1958, Keeling has monitored this change in CO_2 and O_2 concentrations by taking air samples from the atm over several decades and presenting Keeling's curves, which exhibit a saw tooth pattern for both CO_2 and O_2. These saw tooth patterns and the inverse relation between CO_2 and O_2 (i.e., CO_2 increases when O_2 decreases in the atm and vice versa) reveal certain similarities to the *RQ* concept in biology. The biology literature assumes that the energy release per unit mole of oxygen, or higher heating value per unit mole, or Peta mole of oxygen $\{HHV_{O_2}\}$, is constant at about 448 Exa J per Peta mole of O_2 consumed for oxidation. The *RQ* concept was recently extended to engineering literature [6,7]. It was shown that the CO_2 released in giga tons per unit Exa J is equal to $0.1 * RQ$ (more details in Section 3.3.1). This relation was also used to estimate the CO_2 tax per km or mile driven rather than using the weight of the vehicle for taxation as currently done in the EU [6]. The lower the *RQ* (e.g., natural gas with $RQ = 0.5$), the lower the CO_2 emitted, and the higher the *RQ* (e.g., coal, $RQ \approx 1$), the higher the CO_2 emitted for the same energy released. In order to minimize the amount of CO_2 added to the atm, it is of interest to select FF, which has the lowest amount of CO_2 released for fixed energy release.

2. Literature Review

The literature review is divided into the following sections: (i) CO_2 source from FF and other global warming gases, (ii) Keeling's data on CO_2 and O_2 in the atmosphere (atm), (iii) CO_2 and global warming, (iv) CO_2 sources and sinks, O_2 sources and sinks, and models, and (v) the need for current work.

2.1. Fosssil Fuel, Land Use and CO_2

Large quantities of CO_2 released from the combustion of FF (about 87 % of CO_2) play a major role in climate forcing [8]. Further CO_2 is also released due to the land use (LU, 13 %, fire, deforestation, domestic wood consumption, decomposition of dead wood in soil, etc.) by humans. The combined CO_2 from FF and LU will be referred to as CO_2 from FFLU. Global warming gases include CO_2, CH_4, N_2O [9], and chlorofluorocarbons (CFC) with various degrees of global warming potential (GWP). The GWP of biofuels was evaluated by Holtsmark and compared against the impacts of fossil fuels [10]. Biomass and other renewable fuels (e.g., ethanol produced from plant materials), including nutrients consumed by BS, are considered to be carbon neutral, and hence the CO_2 released due to the oxidation of renewable fuels is not considered in the carbon footprint, while the C emitted during the combustion of FF is accounted for in the carbon footprint. Due to anthropogenic activities, each fuel has its own share of global warming, irrespective of

whether the fuel is renewable or non-renewable. For the period 1950–1982, Boden et al. [5] estimated the emission of CO_2 using the fuel production data, and C oxidized to CO_2. The impact of residential energy consumption on GHG emissions and policies that can be implemented to reduce energy utilization were reviewed by Nejat et al. [11].

2.2. Keeling's Data on CO_2 and O_2 and Saw Tooth Pattern

Using monthly data from weather stations close to volcano Mauna Loa, Hawaii (NO AA Global Monitoring Lab, Mauna Loa Observatory (MLO), North flank of Mauna Loa Volcano, Hawaii, elevation: 3397 m above sea level (far from human population) on CO_2 and O_2 (1960–2021), Keeling plotted CO_2 and O_2 vs. year (Figure 1), which is known as Keeling's curve [12,13]. The curves reveal the asynchronous "choreography between atmospheric CO_2 and O_2" and the saw-tooth pattern on CO_2 and O_2. Instead of "per meg" units of Keeling, ppm (4.8 per MEG = 1 ppm) is used for CO_2 concentrations in the current text. Figure 1 reveals a cyclic saw-tooth pattern of small peaks and valleys (note: captions of figures contain more information so that text could be reduced). Balkanski et al. [14] attribute the CO_2 cycle to terrestrial (land) biotic activity. Particularly during fall and winter (FW, Fall: September, October, and November; Winter: December, January, and February), the release of CO_2 due to the combustion of fossil fuels and the sink of oxygen from the atm. dominate the CO_2 sink and O_2 production for the growth of biomass. Thus, during FW, $\Delta CO_2 > 0$ and $\Delta O_2 < 0$. The reverse happens in spring and summer (SS, Spring: March, April, May; Summer: June, July, August); the sink of CO_2 and production of O_2 via biomass growth and limited outgassing of O_2 from the ocean (due to warm temperatures) dominate the CO_2 source and O_2 sink for energy release from power plants, resulting in $\Delta CO_2 < 0$ and $\Delta O_2 > 0$ in SS [15]. The amplitude of CO_2 oscillation is about 6 ppm. The net effect of FW and SS behaviors is positive production of CO_2 per year, resulting in an increase of atmospheric CO_2 in ppm.

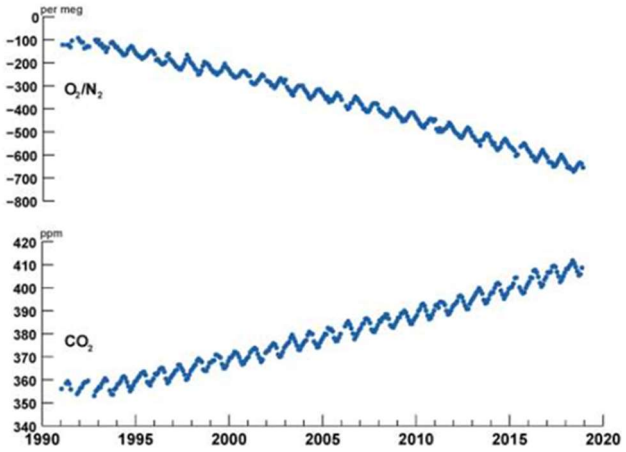

Figure 1. The saw-tooth pattern of CO_2 and O_2 concentrations in earth's atmosphere. Adopted from Ref. [16]. Night-time CO_2 concentration > day-time CO_2 concentration due to photosynthesis during daytime. Change in O_2 expressed as $\delta(O_2/N_2)$ (per meg) by Keeling [16]; they have negative values; O_2 in ppm = per meg units $*$ 0.2096, or 4.8 per megs = 1 ppm of O_2; also see Ref. [17]. Air in atm: 1.77×10^5 Peta Moles. 1 ppm of any species in atm = 0.177 Peta Moles. Between 1960 and 2019, $\delta(O_2/N_2)$ decreased by 700 per meg, implying decrease of 147 ppm of O_2. The referenced oxygen concentration in 1960 was 209,640 ppm. The fluctuations (small peaks and valleys) in CO_2 each year are due to seasonal changes from FW to SS. See data collection [16]. The CO_2 average for 2022 was 417.1 ppm (NOAA). Since 2000, almost 75% of the increase in CO_2 is due to fossil fuel combustion. If the 2021 CO_2 level (415.1 ppm) needs to be restored to the 2000 level (369.7 ppm), one must sequester CO_2 mass of 353 GT.

2.3. CO_2 and Global Warming

The CO_2 record shows that the normal level of CO_2 for centuries was about 300 ppm; however, it reached 414.7 ppm in 2021 and 424 ppm in May 2023 [18]. An increase of 2 ppm of CO_2/year (i.e., almost 15.6 GT of CO_2 added to atm) is related to a global warming rate of 0.0125 °C/year [19]. The synchronous dance between CO_2 and Antarctic temperatures is illustrated in Figure 2, while Figure 3 shows the temperature since 1875. The rising global temperature of the earth is shown to reduce the PS process; hence, by 2040, CO_2 sink due to biomass growth will be reduced by almost 50% [20].

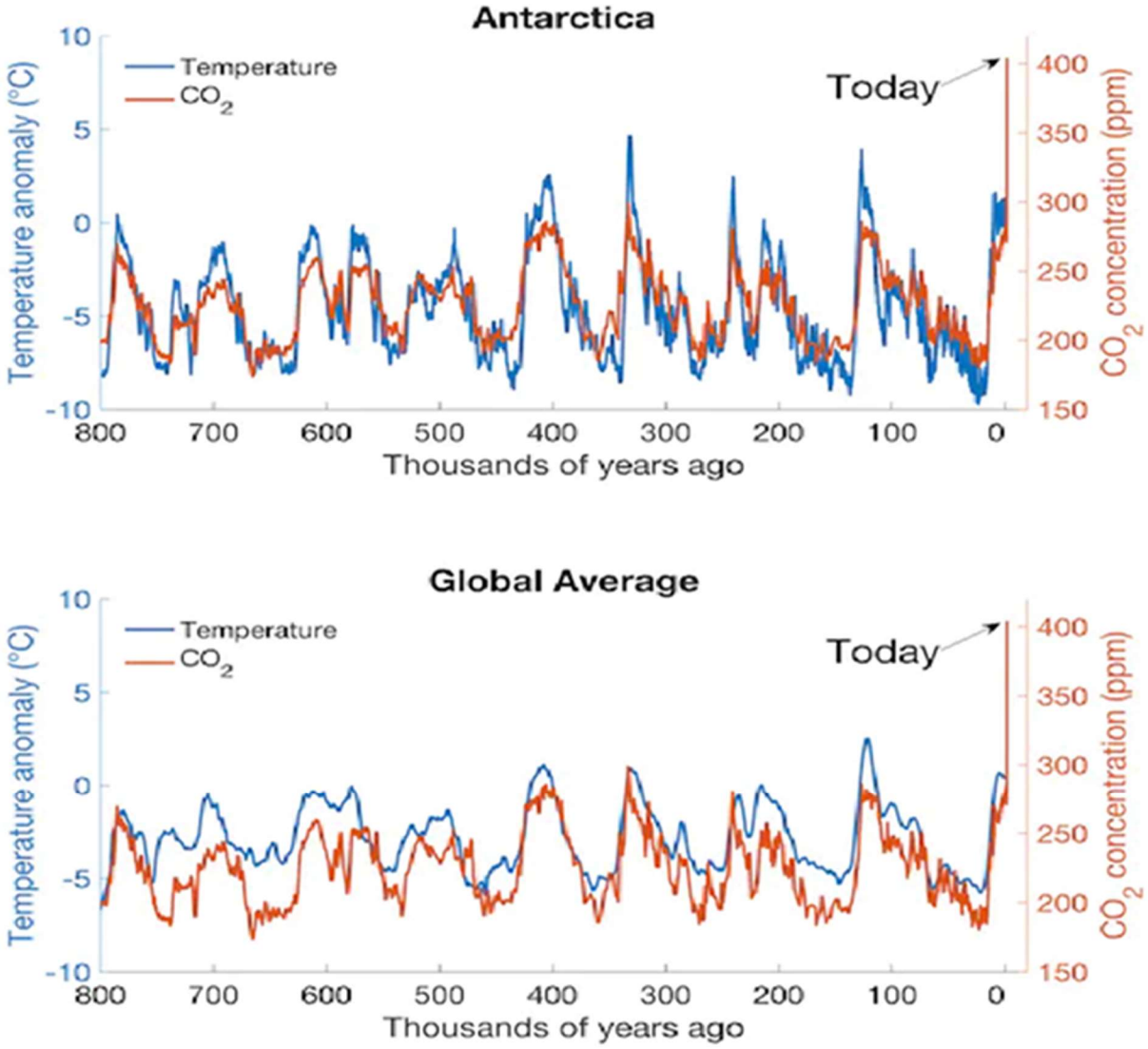

Figure 2. Correlation between CO_2 and atmospheric temperature anomaly (deviation from long-term (30 years) average temperature) in Antarctica (measured from European Project for Ice Coring in Antarctica (EPICA) Dome C ice core sample containing trapped air} and global temperature anomaly; see Ref. [21] for global average surface temperature data. The CO_2 levels fluctuated between 200 and 280 ppm (mean: 240 ppm) for several thousands of years before 2000. The atmospheric temperature fluctuates in synchrony with CO_2 fluctuations for both global average and Antarctica. (Additional Refs: Jouzel et al., 2007 [22]; Lüthi et al. [23]) For records on CO_2 and temperature 800,000 years before the present, see refs. [22–24]. In March 2022, the temperature in Eastern Antarctica spiked by 39 °C (102.2 °F) above the monthly average of −45 °C.

The relationship between CO_2, warming temperature rise, saturation pressure of water vapor, and hence the increasing number of hurricanes, wildfires, etc., is well established [25]. There is also increased seaweed (Sargassum, which smells like rotten eggs–due to hydrogen sulfide) growth due to global warming and rainfall. Assuming ocean temperatures are the same as the global average temperature, the author estimated the variation in saturation pressure, which is shown in Figure 3. Assuming the % increase in hurricanes from 2012 to 2022 is proportional to the % increase in saturation pressure (about 12%). The data from the autopiloted Saildrone Explorer SD 1045 boat indicated a 10% increase in hurricanes and an 8% increase in storms [26], but rain increased only by 1.3% per K rise. The increased ocean temperature will also result in the release of O_2 from oceans (a decrease of 0.2–0.5% per year from oceans). The warmer the ocean, the more vapor in a region and the lesser the barometric pressure, resulting in a higher wind velocity and faster growth of hurricanes [27].

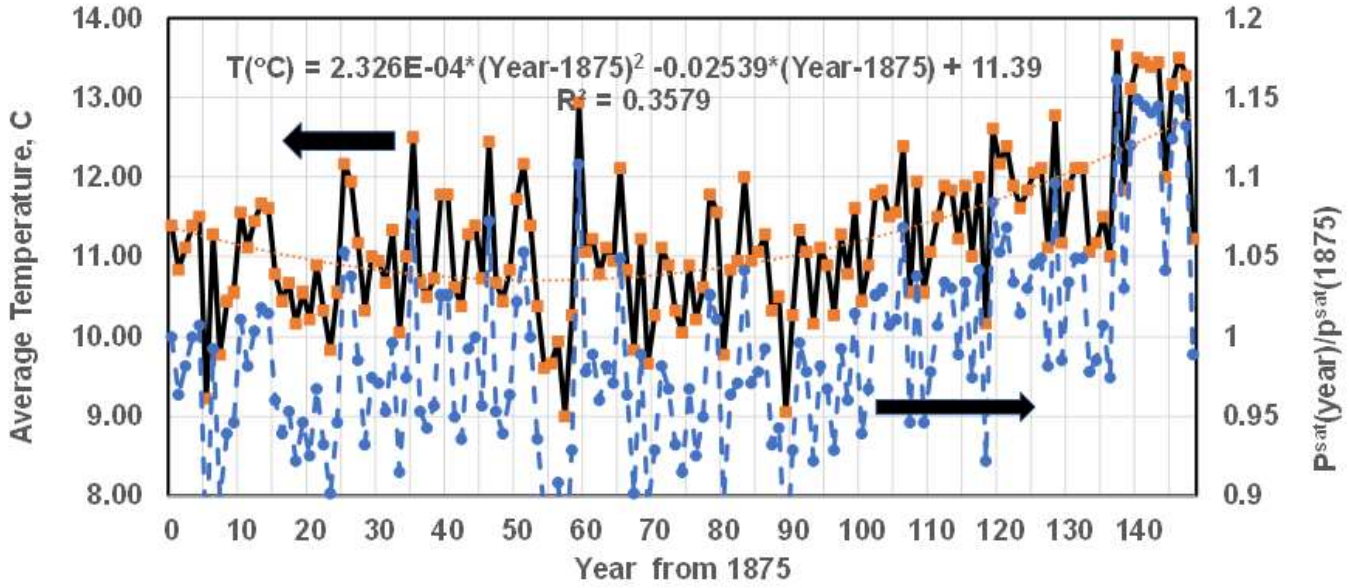

Figure 3. Relation between the global temperature (primary axis, solid line) and the saturation pressure of water (secondary axis, dashed line); temperature data taken from Ref. [28] and pasted onto EXCEL sheet. Global Average T in °C = $2.326 \times 10^{-4} * \text{year}^2 - 0.02539 * \text{year} + 11.39$, Year: (Specified year-1875) P^{sat} by the author using $\ln(P^{sat}) = A - B/(T + D)$, P^{sat} in bar, T in °C, A = 12.22, B = 4120.6, D = 237.9: For 2002, temperature rise per year = 0.044 °C/year, and 0.44 °C/decade. Increasing global temperature causes increasing saturation pressure (P^{sat}); evaporation rate is proportional to P^{sat}.

2.4. CO_2 Sources and Sinks, O_2 Sources and Sinks, and Models

There is extensive literature on CO_2 emissions and CO_2 distribution amongst atm, land, and ocean biomasses and oceans. The CO_2 sinks and O_2 sources are mainly land biomass plants, trees, and ocean PP and CO_2 sinks via ocean storage. Zhu et al. used Integrated Biosphere Simulator or global vegetation model to estimate the effects of climate change and CO_2 fertilization on CO_2 budget at the local subtropical area of China covered with evergreen forest [29].

The global carbon project summarizes several models for the global C budget: (Table 4 in Ref. [30]): (i) Model for CO_2 via land use [31], (ii) Computer model for CO_2 flux from land to atm, CO_2 sink from global vegetation (land-based biomass [32]), which includes growth function models, (iii) Global ocean bio-geochemistry models, and (iv) Ocean CO_2 flux model. Terhaar et al. proposed a new model—An observation-based estimate of ocean carbon sink [33,34]. Gloege et al. modeled ocean uptake by estimating the CO_2 flux across the air-sea interface using iterative global ocean biogeochemical models (GOBMs), which include ocean circulation. For the first guess, they use results from earlier models. Li et al. proposed an emission-driven earth system model for predicting the variations in the

global carbon budget (GCB) [35] and presented variations in the GCB (1970–2018). Yakir et al. summarizes the use of carbonyl sulfide (COS) as a tracer gas to measure changes in CO_2 uptake via PS [36]. To improve the circulation of CO_2 sinks in the ocean, artificial deep-water pumping is recommended, and models are presented in ref. [37].

This model details the capture of CO_2 in terms of C-N-P ratios, particularly for micro- and macro-algae-based biomass in conditions ranging from tropical to subpolar oceans. Li's model of land and oceanic sinks is based on the oxygen budget [38]. Zhu et al. used Integrated Biosphere Simulator or global vegetation model to estimate the effects of climate change and CO_2 fertilization on CO_2 budget at the local subtropical area of China covered with evergreen forest [29]. Control of climate change requires that CO_2 emissions are minimized and CO_2 sinks are maximized, with the ultimate goal of 'net-zero' emissions as per the Paris Agreement [39].

Most of these models require extensive computation tools to estimate CO_2 sinks in GT/year for land and ocean sinks, but they are probably more accurate since they account for temperature, soil conditions, ocean circulation, etc. These models were checked by comparing the results for total CO_2 capture by atm, land and ocean with CO_2 release by FFLU. Hence, there is always a carbon imbalance when CO_2 budget analysis is conducted [40]. None of the literature contains explicit relations for CO_2 sinks amongst the atmosphere, land, and ocean in terms of the *RQ* of FF and BM. Those relations provide (i) the first guess for the iterative models and (ii) the governing parameters that affect CO_2 distributions. Further, the present model uses CO_2 and O_2 balance, and hence there is no C imbalance in the current model. While the NASA website [41] contains curve fits to a saw tooth pattern using a polynomial function (quadratic and cubic) with the addition of a sinusoid with time 't' elapsed in years since 1982, the current work uses the *RQ* method to explain the saw tooth pattern of O_2 given CO_2 data. Thus, the goal of the current work is to make use of Keeling's data on CO_2 and O_2, along with known *RQ* values of FF and land and ocean biomasses to obtain simple, explicit results for CO_2 distribution in GT/year and distribution as a % of total CO_2 released via FFLU. In order to achieve the above goals, Part I provides an overview of the *RQ* concept, a tabulation of the *RQ* values of FF and BM, and a presentation of global *RQ*. Part II presents the CO_2 and O_2 balances and the results for the distribution of CO_2 sinks amongst atm, biomasses (land and ocean), and ocean water.

The specific objectives for Part I, methodology, results, and discussion are briefly summarized below:

(i) Perform a brief overview of *RQ* in biology and engineering and its relation to terms used in conventional CO_2 and photosynthesis (PS) literature, (ii) Relate *RQ* to CO_2 in Giga Tons (GT) per unit energy released, (iii) Use the reported data on CO_2 emissions in GT and fossil energy in Exa J to estimate the *RQ* of the mix of fossil fuels (RQ_{FF}) used worldwide (gas, liquid, and coal), (iv) Use Keeling's data on CO_2 and O_2 in the atm and curve fit the data using linear and quadratic fits, and (v) Define and estimate the global respiratory quotient (RQ_{Glob}) of "breathing" planet earth and its significance for the CO_2 addition to the atm and CO_2 storage in the oceans.

3. Materials and Methods

The methodology consists of the following: (i) the *RQ* concept for CO_2 sources (FF combustion, Section 3.1) and values of *RQ* for FF, which are properties of FF (ii) *RQ* concept for CO_2 sinks (biomasses, Section 3.2), (iii) comparison of *RQ* with terms used in PS literature, (iv) *RQ* values for FF and biomasses and the relations between CO_2 in tons per unit energy release, and *RQ*, (v) *RQ* of FF for CO_2 sources under complete combustion (FF in power plants and automobile engines) and incomplete combustion (oil and gas flares), (vi) Relations between CO_2 in tons per unit energy input and *RQ* of biomass for CO_2 sinks, (vii) RQ_{FFLU} for the CO_2 released from both FF and land use (LU) and *RQ* of a mix of various types of FF, and (viii) definition of Global *RQ* {RQ_{Glob}} for planet earth, a non-property, using Keeling's data. Section 4 presents the results for (i) the *RQ* of the fossil fuel mix used worldwide, (ii) curve fit constants for linear and quadratic fits of Keeling's

data on CO_2 and O_2, and (iii) an estimation of RQ_{Glob}, physical meaning of RQ_{Glob} and its implications on CO_2 emissions in the atmosphere, atmospheric pressure, mass loss of earth due to mining of FF, and prediction of saw tooth pattern of O_2 from given CO_2 data and RQ_{Glob}.

3.1. Respiratory Quotient (RQ) fr CO_2 Sources

3.1.1. Respiratory Quotient (*RQ*)

The biology literature describes the breathing and overall metabolic processes of BS in terms of the respiratory quotient (*RQ*), defined as:

$$RQ_{nut} = \frac{N_{CO_2,nut} =}{N_{O_2,nut}} = \frac{N_{C,nut}}{N_{O_2,nut}} \quad (1)$$

where RQ_{nut} is the *RQ* of nutrient s a property, $N_{CO_2,nut}$ is the number of moles of CO_2 released when nutrient is oxidized, $N_{C,nut}$ is the number of C atoms in the nutrient, and $N_{O2,nut}$ is the number of moles of O_2 used in oxidation.

Caution: a few of the references in both biology and CO_2 literature (e.g., [42,43]) use the inverse definition (i.e., O_2 moles used/CO_2 moles released) for the *RQ*, and the results in those manuscripts must be interpreted accordingly. For humans or any BS-oxidizing nutrients (glucose $C_6H_{12}O_6$, carbohydrate (CH), fat (F), and proteins (P)) produced by the digestive system from food intake, the *RQ* can be estimated from the chemical formula of the three nutrients [44]:

$$C_6H_{12}O_6 + 6\ O_2 \rightarrow 6\ CO_2 + 6\ H_2O,\ HHV_{O2} = 469\ kJ/mole\ O_2,\ RQ = 1 \quad (2)$$

Dividing by 6, one can write the above equation on a unit carbon formula (UCF) basis:

$$CH_2O + 1\ O_2 \rightarrow 1\ CO_2 + 1\ H_2O,\ HHV_{O_2} = 469\ kJ/mole\ O_2,\ RQ = 1 \quad (3)$$

with UCF represented by CH_2O, the higher heating value of fuel (HHV) = 2813 kJ/mole of $C_6H_{12}O_6$ or HHV = 402.3.1 kJ/mole of CH_2O, HHV_{O2}, the energy released per mole of O_2 used = 2813/6 = 469 kJ per mole of O_2. The =*RQ* of 1 for glucose indicates that 1 mole of CO_2 is released for every mole of O_2 used in the oxidation of CH within the body of BS. For the oxidation of fat ($C_{16}H_{32}O_2$), $RQ = 0.7$. Humans use a mix of CH ($RQ = 1$) and F ($RQ = 0.7$); hence, typically, $0.7 \leq RQ \leq 1$ for a mix of nutrients metabolized. On the other hand, the *RQ* can also be determined from the analysis of nasal exhaust gas (or automobile exhaust gas); hence, one can determine the % of fat oxidized in the mix of CH and F [45]. The same methodology is adopted for the *RQ* of thermal power plants when a mix of natural gas, oil, and coal is used globally. For internal combustion engines (automobiles, gas turbines, etc.) fired with any HC liquid fuels or HC mixed with ethanol, the exhaust gas can yield *RQ* values [7]. Note that *RQ*, as defined in Equation (1), is a property of fuel whe fuel is used in a thermal system.

3.1.2. Significance of Respiratory Quotient (*RQ*) and *RQ* Values for Nutrients and Fuels

Why is *RQ* important for humans and planet earth? The CO_2 released from the metabolism of nutrients in the cells of various organs within a human is collected by the bloodstream, which transfers CO_2 to alveoli in the lungs for eventual nasal exhaust. Typically, the normal CO_2 in veins is at partial pressure p_{CO2} (40 mm Hg or 1.2 milli-moles/L). Thus, for seniors with respiratory acidosis (when all CO_2 cannot be breathed out, the blood becomes acidic due to CO_2 storage exceeding 1.3 milli mole/L) with higher levels of p_{CO2}, a diet with a low *RQ* (i.e., fat [46]) is recommended [47–51]. Note that during acidosis, the *RQ* of nasal exhaust (RQ_{vent} = CO_2 ventilated/O_2 consumed) is a non-property < RQ_{nut}, which is normally about 0.8. While RQ_{nut} is a property of a nutrient or mix of nutrients that can be tabulated (e.g., Table 1), RQ_{vent} is not since it depends upon blood capacity and, hence, how much CO_2 is stored by the blood.

Table 1. *RQ* of Fossil fuels and Biomasses represented by Chemical formula CH_hO_o. Gasoline CO_2 in kg per gal = 13.2; *RQ* for gasoline with HHV of gasoline 0.132 GJ/gal. Gasoline CO_2 in lb. per gal = 29; *RQ* for gasoline with HHV of gasoline 0.125 MMBtu/gal.

Fuel	"h" or H/C	"o" or O/C,	*RQ*	HHV (kJ/kg) [1]
Wyoming coal	0.70	0.18	0.92	18,347
Gasoline (C_8H_{18}), Y_C = 0.85, ρ = 0.75 kg/L	2.25	0.00	0.64	47,968
Diesel ($C_{12}H_{23}$), ρ = 0.84 kg/L	1.92	0.00	0.68	46,350
#6 low S fuel oils	0.12	0	0.73	42,900
Methane CH_4	4.00	0.00	0.50	55,426
Organic acid (e.g., malic acid, $C_4H_6O_5$) M = 134.1	1.5	1.25	1.33	9993
Sargassum [2] (seaweed), $CH_{1.74}N_{0.025}O_{1.42}S_{0.018}$.	1.74	1.42	1.57	20,120 (DAF)
Human Body wet (60% H2O, 40% dry) {$C_{1.54}H_{3.24}N_{0.228}O_{0.733,}$ $Ca_{0.037}P_{0.032}$}.3.33 H_2O(l), or {1.54 $CH_{2.1}N_{0.15}O_{0.48}Ca_{0.024}P_{0.021}$}. 3.33 H_2O(l) based on Ultimate analysis in Ref [52]	2.1	0.48	0.76	23,500 (Boie, dry, no P oxid)
Generic PP: $C_x(H_2O)_w$ $(NH_3)_yH_zH_3PO_4$ (a) Without Nitrification (b) With Nitrification	{3 + 2w + 3y + z}/x {3 + 2w + 3y + z}/x	(w + 4)/x (w + 4)/x	1 + (1/4)(z/x) 1 + 2(y/x) + (1/4)(z/x)	
Ocean Plankton $C_xH_{2w+3y+z+3}N_yO_4P$, [53]			x/{x + 2y + z/4)	
Planktonic marine algae [3]: Redfield–Ketchum–Richards Formula: C_{106} H_{263} O_{110} N_{16} P [53]; x = 106, y = 16, w = 106, C_{106} H_{263} O_{110} N_{16} P + 138 0_2 = 106 CO_2 + 16 HN03 + H3P04 + 12_2 H2O *RQ* = 0.72 to 1.11 Note 1	2.481	1.038	0.77, 0.7_2 to 1.11 with an average of 0.82 [54]	
Keeling land vegetation via PS and respiration [55]			0.95 (land)	
Carbo-hydrate, CH (e.g., glucose) $C_6H_{12}O_6$ or CH_2O or sugars	1.0	1.0	1.0	
Fats $C_{16}H_{32}O_2$ [7]	2.0	0.1	0.7	
Lipids: $C_{40}H_{74}O_5$	1.85	0.125	0.73 or 0.68–0.8 [56]	
PProteins, $C_{4.57}H_{9.03}N_{1.27}O_{2.25}S_{0.046}$ [45]	1.98	0.49	0.8–0.9, see also [56]	

Note 1: The histogram in Ref. [57] suggests *RQ* from 0.6 to 0.9 as the maximum number of occurrences, while *RQ* ranges from 0.3 to 3.1 [57]. The same Ref. seems to suggest *RQ* < 1, since *RQ* = 1/{1 + 0.25 ∗ (H/C) − 0.5 ∗ (O/C) + 1.25 ∗ (N/C) + 1.25 ∗ (P/C)} [58]. [1] Divide the units of kJ/kg by 2.205 to obtain BTU/lbm, and kJ/mole by 2.32 to obtain BTU/lbmole. [2] Sargassum, data based on ultimate analyses reported in [59]. [3] Ref. [60] reports chemical composition of various kinds of phytoplankton: diatoms, other autotrophs, heterotrophs, detritus, and most of them have very similar atom ratios. On average, $CH_{1.66}N_{0.15}O_{0.56}P_{0.014}Si_{0.046}$, O_2 st = 1.15 moles, *RQ* = 0.87.

A similar problem exists for the "breathing but aging planet", with human activities resulting in CO_2 release from FF into the atm and increasing storage of CO_2 by oceans. So, for the same energy needs, stoichiometric O_2 consumption is fixed for most FF (natural gas, oil, coal), and hence low *RQ* fuels generate less CO_2 per unit energy. The FF with high *RQ* values generates more CO_2, which results in increased storage of CO_2 in the oceans, called the "lifeblood of the earth" [61], making them more acidic (i.e., less pH) [62], and affecting the growth of PP and, hence, the release of O_2 from the oceans. Thus, with increasing CO_2 in the atm, the earth needs FF with lower *RQ* values [7] (e.g., CH_4 or natural gas with *RQ* = 0.5), just like doctors recommend a low-*RQ* diet for seniors.

The *RQ* values under complete oxidation and HHV for limited fuels, including fossil fuels (FF) and nutrients, are presented in Table 1. The *RQ* values indicate that the impact of FF (gas, oil, and coal) on emissions of CO_2 is not equal. Coals typically have values close to 1, while natural gas (mostly CH_4) has low *RQ* values at 0.5 [7].

3.2. Respiratory Quotient (RQ), Redfield Ratio (RR), Exchange Ratio (ExRExR), Photosynthetic Quotient (PQ) for CO_2 Sinks

Photosynthesis (PS) is a process in which CO_2 and H2O react to produce C-rich biomass (typically C-H-O) and O_2 with energy input from the sun. Compared to combustion of FF or biomass (e.g., CH_2O is also a biomass, Equation (3)), where CO_2 is a source and O_2 is a sink with energy release, biomass growth serves as a CO_2 sink and an O_2 source with energy input from sun. For biomass CH_2O(s) growth via PS, one may use the inverse of the oxidation reaction (Equation (2)), given by:

$$6CO_2 + 6H_2O \rightarrow, C_6H_{12}O_6, + 6O_2, RQ_{BM} = 1 \quad (4)$$

On a UCF basis, one may divide Equation (4) by (6), and hence

$$CO_2 + H_2O \rightarrow CH_2O(s) + O_2, 469 \text{ kJ input per mole of } O_2, RQ_{BM} = 1 \quad (5)$$

which is the inverse of Equation (3). CH_2O is one type of biomass. Each mole of CO_2 sinks results in the addition of one mole of C to biomass and one mole of release of O_2. Thus, 1 mole of O_2 requires 469 kJ per mole of O_2 production; this number varies within a narrow range and is almost constant for any fuel or biomass. For biomass growth under PS, the global warming literature uses various terms: *RR*, *PQ*, *ExR*, and regeneration quotient (*RgQ*) [14], which are defined as

$$PQ_{BM} = ExR_{BM} = RR_{BM} = (RgQ)_{BM} = \frac{N_{O_2,BM}}{N_{CO_2,BM}} = \frac{N_{O_2,BM}}{N_{C,BM}} = \frac{1}{RQ_{BM}} \quad (6)$$

where RR_{BM}, the *RR* of biomass, and *ExR* is Keeling's exchange ratio. The RQ_{BM} is defined as

$$RQ_{BM} = \frac{N_{CO_2,BM}}{N_{O_2,BM}} = \frac{N_{C,BM}}{N_{O_2,BM}} \quad (7)$$

where $N_{CO_2,BM}$ is the net CO_2 moles consumed by any biomass {=CO_2 consumed -CO_2 used in respiration} in the conversion to organic matter, and similarly, $N_{O2,BM}$ is the net O_2, moles produced = {O_2 produced via PS—O_2 used in respiration}. Note that when RQ_{BM} = 1, $RR_{BM} = PQ_{BM} = (ExR)_{BM} = (RgQ)_{BM}$ = 1 [42].

Mann et al. presented the average composition of marine organic matter (MOM; P:N:C:O_2 = 1:16:106:138 [63]) and RQ_{MOM} [43]. For the given MOM composition, RQ_{MOM} = 0.768 or *RR* = 1.3 (a value close to fat in BS). For ocean biomass (Table 1), *RR* = 150 mol of O_2 produced/106 mol of CO_2 fixed = 1.41 [59], RQ_{BM} = 0.71.

For estimating the *RQ* of biomasses and coals, the ultimate analyses are first converted into a chemical formula on a UCF basis ($CH_hN_nO_0S_s$), where h = H/C, N/C, o = O/C ratio, and s = S/C, etc., and then the *RQ* is estimated using the empirical chemical formula: {$1/(1 + h/5\text{-}o/_2 + s)$}. For most land-based biomass, $RQ_{LMB} \approx 1$ {(LBM), Appendix A.1}.

The PQ and RQ_{OWBM} values for ocean water biomasses (OWBM) are known to vary from 1.0 to 1.8 {RQ_{OWBM} from 0.55 to 1} in the Southern Ocean and 1.0 to 1.4 {RQ_{OWBM} from 0.72 to 1} in non-polar oceanic areas. The average value of RQ_{OWBM} = 0.8, or PQ = 1.25 [64]. Ref. [57] reports that the various PP groups in oceans have an $\{RQ_{OWBM}\}_{median} \approx 0.88$ and an RQ average of 1.11. Marino et al. demonstrated that oxygen concentrations in oceans and hence the carbon sink in a biome depend strongly on the RR (RQ. Based on a review in Ref. [57], the RQ of marine PP respiration assumes a constant value of RQ_{OWBM} = 0.8. These values will be used in Part II to obtain the carbon budget and distribution amongst the atmosphere, land and ocean biomasses, and ocean storage.

3.3. Relation between Respiratory Quotient (RQ) and CO_2 Released in Tons for CO_2 Sources

For carbon sources, the CO_2 in GT per Exa J of energy output (for CO_2 sources) or input (for CO_2 sinks) is obtained in terms of RQ values.

3.3.1. CO_2 Sources

Consider the combustion of FF, which is a CO_2 source, and the definition of RQ. With constant HHV_{O2}, each Exa J of energy released by FF requires $\{1/HHV_{O_2}\}$ Peta moles of O_2. Thus, CO_2 in Peta moles released per Exa J of energy = $RQ * \{1/HHVO_2\}$. Using the molecular weight of CO_2,

$$CO_2, \left(\frac{GT}{ExaJ}\right) = \frac{M_{CO_2}}{HHV_{O_2}} RQ = 0.1 \ * \ RQ \ , \frac{M_{CO_2}}{HHV_{O_2}} \approx 0.1 \tag{8}$$

where M_{CO_2} = 44.01 g/mole = 44.01 GT/Peta mole and HHV_{O2} = 448 Exa J/Peta mole of O_2. This value of 448 Exa J/Peta mole of O_2 yields was cross-checked by estimating the energy released as 112 Exa J per electron mole transfer, where the number of electron mole transfer = 4 ∗ stoichiometric moles [65]. This number checks with the value of 111.1 Exa J per Peta electron mole transfer used in biology literature [66]. If the approximation of constant HHV_{O2} is not used and if measured heating values (MJ/kg fuel) are used for well-known C-H-O fuels (e.g., hydrocarbons, alcohols, aromatics, coal, and biomasses with known empirical chemical formula), the CO_2 in GT/Exa J and RQ can be directly estimated. The plot of CO_2 in GT/Exa J vs. RQ reveals almost the same slope as 0.1 (Figure 4). See Ref. [7] and the caption of Figure 4 for more details. Selecting English units,

$$CO_2, \left(\frac{Tons}{MMBtu}\right) = 0.116 \ * \ RQ \tag{9}$$

Since C in tons = CO_2 in tons ∗ 12.01/44.01 = 0.27 ∗ CO_2 in tons, then Equations (8) and (9) become:

$$C, \left(\frac{GT}{ExaJ}\right) = 0.027 \ * \ RQ \tag{10}$$

$$C, \left(\frac{Tons}{MMBtu}\right) = 0.032 \ * \ RQ \tag{11}$$

It is seen that for coals dominated by C atoms (Table 1), $RQ \approx 1$, and hence CO_2 in GT per Exa J = 0.1 (or 0.116 short tons per MMBtu), while for CH_4 (or natural gas), it is only 0.05 Giga Tons per Exa J.

The higher the RQ values of FF fuels, the more CO_2 or C in Giga Tons per Exa J of energy is released. On the other hand, if CO_2 in Giga Tons per Exa J is known for a mix of fossil fuels (natural gas, fuel oil, coal, etc.), then the RQ of the mix can be determined (See Section 3.4.1 for more details).

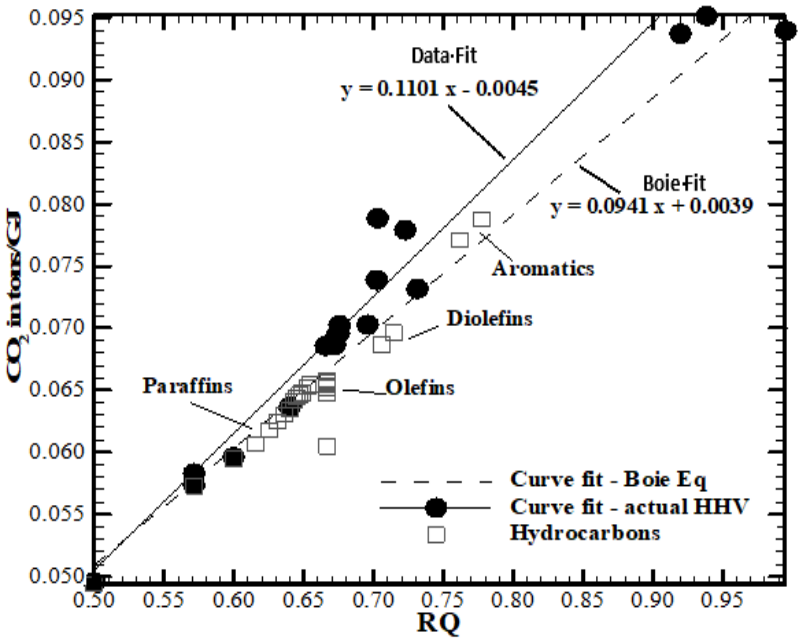

Figure 4. Variation of CO_2 emitted in tons per GJ of energy released (or Giga Tons per Exa J) for fuels with *RQ* of fuels. Figure adopted from [7]. Measured heating value and composition data were used to estimate the CO_2 released in tons per GJ and *RQ* of fuels. The sloped values are compared with the slope obtained from the use of empirical Boie equation for gross or higher heating value (HHV) kJ/kg of fuel = {35,160 Y_C + 116225 $*$ Y_H − 11,090 $*$ Y_O + 6280 Y_N + 10,465 Y_S, where Y_C, Y_H, Y_N, Y_O, and Y_S are mass fractions of carbon, hydrogen, nitrogen, oxygen, and sulfur in a C-H-N-O-S fuel. The slopes of both trend lines were approximately 0.1.

3.3.2. *RQ* for Incomplete Combustion

The *RQ* values listed in Table 1 and the CO_2 tons per GJ relations in Equations (8)–(11) are best suited for fuels undergoing complete oxidation for applications focused on energy conversion to work. However, *RQ*'s and Equations (8)–(11) may not be suitable for fuels undergoing moderate to severe incomplete combustion. Consider the release of pure CH_4 from cattle feedlots and the incomplete oxidation of flare gas near oil fields and refineries with CO_2 and CH_4 released into the atm. CH_4 is also a global warming gas, but with a CO_{2eq} of around 10.4 (i.e., 10.4 times more potent than CO_2 in causing global warming on a mole basis and a 28.5 mass basis called GWP). For these cases, the *RQ* is estimated by using the following relation:

$$RQ_{Glob,CO2+CH4} = \frac{\{[CO_2] + [CH_4] \ * \ GWP\}_{atm}}{\{[O_2]\}_{atm}}, GWP \ for \ CH_4 = 10.4 \tag{12}$$

where $[CO_2]$, $[O_2]$, and $[CH_4]$ are concentrations in ppm. If pure CH_4 production in moles/year (=1000 $*$ volume in SCM per year/24.5 or 1.159 $*$ SCF or CH_4 mass in g per year/16.05) is known, then

$$\begin{aligned} CO_2 \ eq \left(\frac{GT}{year}\right) &= \frac{CO_{2,eq} * 1000 * 44.01}{\{24.5 * 10^{15}\}} * \dot{V}_{CH_4} \\ &= C_{SI} \ * \ CO_{2,eq} * \dot{V}_{CH_4}, C_{SI} = 1.7963 \ * \ 10^{-12} \end{aligned} \tag{13}$$

where $\dot{V}_{CH_4}$ is volume flow rate in SCM per year

$$CO_2eq \left(\frac{GT}{year}\right) = C_{Eng} \ * \ CO_2eq * \ \dot{V}_{CH_4}, \ C_{Eng} = 4.8991 \ * \ 10^{-12} \tag{14}$$

where $\dot{V}_{CH_4}$ is volume flow rate in SCF per year. Natural gas flaring is the combustion of natural gas (≈CH_4) typically associated with oil extraction. Even though the CH_4 flaring has negative environmental effects, the transport of gas is not cost-effective due to a lack of gas pipelines. The average combustion efficiency is 91%, including lit and unlit (3–5%) periods, malfunction, and incomplete combustion [67]. For the gas flares,

$$CO_2\left(\frac{GT}{year}\right) = C_{SI} * \eta * \dot{V}_{CH_4}, \; C_{SI} = \frac{1000 * 44.01}{24.5 * 10^{15}} = 1.796 * 10^{-12} \tag{15}$$

$$CO_2\left(\frac{GT}{year}\right) = C_{Eng} * \eta * \dot{V}_{CH_4}, \; C_{Eng} = 5.0966 * 10^{-14} \tag{16}$$

where η is the burned or oxidized fraction of CH_4.

$$CO_2, eq\left(\frac{GT}{year}\right) = C_{SI} * (1-\eta) * CO_2, eq * \dot{V}_{CH_4}, \; C_{SI} = 1.7963 * 10^{-12} \tag{17}$$

$$CO_2, eq\left(\frac{GT}{year}\right) = C_{Eng} * (1-\eta) * CO_2, eq * \dot{V}_{CH_4}, \; C_{Eng} = 5.0966 * 10^{-14} \tag{18}$$

$$CO_2, \left(\frac{GT}{year}\right) = C_{SI} * \dot{V}_{CH_4}\{\eta + (1-\eta) * CO_{2,eq}\} \tag{19}$$

According to the World Bank's global gas flaring tracker for 2021, about 140 Giga SCM of natural gas was flared, which releases almost 5 Exa J of energy per year when burned completely. Thus, if 100% is burned, then CO_2 emission is 0.25 GT of CO_2 (which checks with the relation given by Equation (8) with RQ = 0.5 and energy release = 5 Exa J/year). If 0% is burned, then with a $CO_{2\,eq}$ of 10.4, the CO_2 eq emission for CH_4 is 2.62 GT/year. If 90% is burned and 10% is unburned, then a total of 0.49 GT of CO_2/year (=0.25 ∗ 0.9+ 0.1 ∗ 2.62, Equation (19)), which checks with World Bank data, but 0.47 GT of CO_2 equivalent is released.

3.3.3. RQ for CO_2 Sinks and GT of CO_2 Sink per Unit Energy Input

Land and ocean biomasses serve as CO_2 sinks and O_2 sources. The biomass term is generalized to include terrestrial (land), ocean water, or marine-based biomass and microorganisms. For these CO_2 sinks, Equations (8)–(11) can be equally applied, and in this case, they represent the CO_2 sink per unit energy input reaching the chlorophyll via PS. Replacing RQ by RQ of growing biomass, RQ_{BM},

$$\begin{aligned} CO_2\left(\tfrac{GT}{Exa\ J}\right) &= 0.1 * RQ_{BM} \\ CO_2\left(\tfrac{GT}{MMBtu}\right) &= 0.116 * RQ_{BM} \end{aligned} \tag{20}$$

$$\begin{aligned} C\left(\tfrac{GT}{Exa\ J}\right) &= 0.027 * RQ_{BM} \\ C\left(\tfrac{shortTon}{MMBtu}\right) &= 0.032 * RQ_{BM} \end{aligned} \tag{21}$$

It is assumed that the RQ_{BM} during growth is the same as the RQ_{BM} during the oxidation process; see also Ref. [17], which presumes that the RQ_{BM} = 1. If $\dot{C}$(s) sink data in GT/year are available for biomass, then CO_2 in GT/year = 3.667 ∗ C(s) in GT/year and CO_2 moles per year = (1/12.01) ∗ $\dot{C}$(s). The O_2 moles produced per year = (1/12.01) ∗ $\dot{C}$(s)/RQ_{BM}. If biomass happens to be C(s) or CH_2O(s), RQ_{BM} = 1. The ocean RQ_{OWBM} has a small spatial variability consistent with previous data [58], and the mean RQ_{OWBM} is around 0.7. It is seen in Part II that the RQ of combined land and ocean water-based biomasses is dominated by LBM since net O_2 added to atm. is dominated by land-based biomass.

Consider the ocean biomasses, which serves as a CO_2 sink. For PP,

1. Generic PP: $C_x(H_2O)_w\ (NH_3)_yH_zH_3PO_4$ or $C_xH_{3+2w+3y+z}\ N_y\ O_{w+4}\ P$

Oxidation Reaction: $C_xH_{3+2w+3y+z}\ N_y\ O_{w+4}\ P + \{x + (1/4)\ z\}\ O_2 \rightarrow xCO_2 + y\ NH_3 + H_3PO_4 + \{w + (½)\ z\}H_2O$, without nitrification

Nitrification reaction, $NH_3 + 2O_2 \rightarrow HNO_3 + H_2O$

Overall reaction

$C_xH_{3+2w+3y+z}\ N_y\ O_{w+4}\ P + \{x + 2y + (1/4)\ z\}\ O_2 \rightarrow xCO_2 + y\ HNO_3 + H_3PO_4 + \{w + y + (½)\ z)\}H_2O$

(i) The ocean plants growth via photosynthesis: (See Table 1) is given by,

$$106\ CO_2 + 16\ NO_3^- + H_2PO_4^- + 17\ H^+ \rightarrow C_{106}H_{263}O_{110}N_{16}\ P + 138\ O_2,$$

$$RQ_{OWBM} = \{106/138\} = 0.77,$$

(ii) Planktonic marine algae: The Redfield–Ketchum–Richards Formula is given as $(CH_2O)_{106}(NH_3)_{16}\ (H_3PO_4)$, or $C_{106}\ H_{263}\ O_{110}\ N_{16}\ P$ **[53]** and M = 3553.3 g/mol. Thus, x = 106, y = 16, and w = 106. The *RQ* is estimated at 0.77. For the *RQ* based on the traditional Redfield–Ketchum–Richards equation and algae production, see Refs. [43,68].

(iii) Oceanic cyanobacteria and algae: photosynthesis and respiration, *RQ* = 0.77 [37].

2. Seaweed or Sargassum: A bright seaweed also absorbs CO_2 and produces O_2, but it reflects more of the sun's radiation compared to PP. Using the ultimate analyses reported in [7,69], the chemical formula on the UCF basis is given as $CH_{1.74}N_{0.025}O_{1.42}S_{0.018}$ (See Table A1, Appendix A.1). Thus, for seaweed, $RQ_{BM} = 1.57$, which is unusually high compared to land-based biomasses. It serves as a good CO_2 sink but decomposes and releases NH_3 and H_2S (odors like rotten eggs) along with CO_2. For different seaweeds, Ref. [69] presents ultimate analyses; the author determined the chemical formula and estimated that the *RQ* of seaweeds could vary from 0.95 to 1.34 (Appendix A.1). The measured *RQ* values are from 0.99 to 2.38 (or PQ from 0.42 to 1.01), while the theoretical values are from 0.77 to 1 (*PQ* from 1.0 to 1.3) [70].

3.4. Respiratory Quotient (RQ) of Fossil Fuels and Biomass

3.4.1. *RQ* of Fossil Fuels (FF)

The *RQ* can be readily determined for fuels with known chemical formulas. For many solid fuels, ultimate analyses are available (e.g., coal, biomass) and they can be used to derive UCF [7]. When coal, oil, and gas are used as fossil fuels globally, and if % energy delivered is known, then the *RQ* of this mixture of fuels (RQ_{FF}) can be determined. Two methods are suggested for determin0ng RQ_{FF} of a mix of FF.

Method I: Use reported data on global CO_2 in GT/year and reported annual fossil energy release in Exa J per year [40], then compute GT per Exa J, and use Equation (8) for an estimation of the RQ_{FF}.

Method II: Use the *RQ* values of gas, liquid, and solid fuels (FF) listed in Table 1. $RQ_{gas} = 0.5$ (CH_4 or natural gas), $RQ_{oil} = 0.73$ (# 6 Fuel oil low S), $RQ_{coal} \approx 1$, estimate their energy fractions (EF) from the global data presented and use the formula $RQ_{FF} = RQ_{gas} * EF_{gas} + RQ_{liq}\ EF_{oil} + RQ_{coal} * EF_{coal}$ [7]. Note that the global RQ_{FF} will keep changing depending on the energy fractions of coal, gas, and oil.

3.4.2. Respiratory Quotient for the Combined Fossil and Land Use (LU) CO_2 (RQ_{FFLU})

In addition to CO_2 from FF [71–73], land use (LU) (e.g., cutting down forests and burning, soil degradation, fire, clearing lands for agriculture, etc.) also releases CO_2. In addition to ref. [21] see also the carbon dioxide information analysis center, for anthropogenic emissions. For the years 2007–2016, LU energy accounted for 13% of anthropogenic CO_2 emissions. The land use in 2016 contributed CO_2 of 5.6 GT, while the contribution from fossil combustion amounts to 35.4 GT of CO_2 [73]. Also see *2020 Special Reports: Land Use, Land-Use Change, and Forestry* [74]. The major fraction of CO_2 emitted is from FF > 0.8, and the land use energy fraction for $CO_2 \leq 0.2$. The combination of FF and LU is represented

by the acronym FFLU, which includes CO_2 contributed by both FF and land use (LU). It is noted that FF is the dominant source of CO_2. Thus, the *RQ* for combined FF and LU is defined as

$$RQ_{FFLU} = \frac{N_{CO_2,FFLU}}{N_{O_2,FFLU}} \tag{22}$$

where $N_{CO_2,FFLU}$, CO_2 released by FFLU, and O_2 consumed by FFLU. Thus, the *RQ* of fossil fuel (RQ_{FF}) and the *RQ* from land use (RQ_{LU}) are combined to yield an effective RQ_{FFLU} [7]:

$$RQ_{FFLU} = RQ_{FF} * EF_{FF} + RQ_{LU} * EF_{LU} * RQ \tag{23}$$

where EF_k is the energy fraction contributed by fuel k, which same as is ratio of oxygen consumed by fuel k to total oxygen consumed for fuel mix. Ref [7] shows that EF_k contributed by fuel k is the same as the ratio of O_2 consumed by fuel k to the total O_2 consumed by all fuel types due to the constancy of HHV_{O_2}. RQ_{FF} = 0.73–0.78 and the land use $EF_{LU} \approx 0.2$. For LU, RQ_{LU} is set at 1 when estimating RQ_{FFLU}.

3.5. Global Respiratory Quotient (RQ_{Glob}) for Planet Earth

The breathing systems within the green planet earth include power plants (NBS, CO_2 "exhaled" and air/O_2 "inhaled"), humans (BS, CO_2 "exhaled" and air/O_2 "inhaled"), and biomass on land and in the ocean (BS, CO_2 "inhaled" and O_2 "exhaled"). As summarized in previous sections, the net CO_2 mol added to the atmosphere is the difference between CO_2 released by FFLU and the sum of CO_2 sinks via biomass and ocean storage, and the O_2 mols depleted from the atm is the difference between O_2 mols consumed by FFLU and O_2 mols produced by biomass. Following the *RQ* definition used for FF, the global respiratory quotient of planet earth {RQ_{Glob}} is defined as

$$RQ_{Glob} = \left(\frac{\left\{ \frac{d[CO_2]}{dt} \right\}_{atm}}{\left| \frac{d[O_2]}{dt} \right|_{atm}} \right) \tag{24}$$

where $[d\{CO_2\}/dt]_{atm}$ (ppm/year, positive) represents the net CO_2 added to the atm per year {i.e., the slope of CO_2 vs. year} and the net O_2 depleted from the atm per year $[d\{O_2\}/dt]_{atm}$, slope of O_2 vs. year in ppm/year, usually negative}. Both slopes can be readily evaluated from linear and quadratic curve fits for Keeling's data on CO_2 and O_2 concentration in the atm.

3.6. Data

For presenting the quantitative results on all *RQ*'s and RQ_{Glob}, the following data are required:

(i). Annual fossil and land use energy or annual C or CO_2 emission data for FF and LU. Reported data on CO_2 are in GT/year and fossil energy consumption in Exa J/year. Data are selected from the carbon dioxide and information analysis center (CDIAC) [71–75]. This method is termed Method I.

(ii) With global energy release data for each fuel type (gas, oil, and coal) and determining the fraction of energy contributed by these three types of FF [76], and the *RQ* values of gas, oil, and coal (Table 1) and Equation (23), the RQ_{FF} can be estimated. This method is termed Method II.

(iii) Respiration Quotient for FF (RQ_{FF}) and LU (RQ_{LU}), RQ_{LBM}, and RQ_{OWBM}.

(iv) Curve fit constants for linear and quadratic fits of Keeling's data on CO_2 and O_2 vs. years.

See column 3 of Table 2 for a listing of all formulas and a listing of data for quantitative evaluations.

$$\dot{N}_{O_2,FF} = \left(\frac{\dot{E}_{FFLU}}{HHV_{O2}} \right) = 2.232 * 10^{-3} * \dot{E}_{FFLU}$$

where, $\dot{N}_{O_2,FF}$, oxygen consumed in Peta moles per year; $\dot{E}_{FFLU}$ annual energy consumption by FFLU (Exa J/year). Other necessary data are presented below Table 2 caption.

Table 2. List of formulas for *RQ* and other estimations for linear and quadratic curve fits for Keeling's curves.

Parameter of Interest	Linear Fit	Quadratic Fit
CO_2 in atm., ppm	$a_1 * years + a_0$, linear fit, *years* = current year-1991 a_1 = 2.082 ppm /year, a_0 = 350.5 ppm, R^2 = 0.9709 when all data (multiple data within a year) was used {Fit: 381.7 ppm in 2006, Data in 2006 (average): 381.5 ppm} (average)	$c_2 * years^2 + c_1 * years + c_0$, *years = current year-1991* c_2 = 0.01889, c_1 = 1.473, c_0 = 354.1, R^2 = 0.9804 when all data (multiple data within a year) was used Fit: 380.5 ppm in 2006, data in 2006: 381.5}
O_2 in atm., ppm	$b_1 * years + b_0$ b_1 = −4.438 ppm/year, b_0 = 209488, R^2 = 0.9839 {Fit O_2: 209,421, Data O_2 = 209,423 ppm}	$d_2 * years^2 + d_1 * years + d_0$, d_2 = −0.04347265 ppm/year^2, $d_1 = -3.033_2$ ppm/year., d_0 = 209,480 ppm, R^2 = 0.9896, {Fit O_2: 209,425, with no of years since 1991 = 15, data O_2 = 209,423 ppm}
d[CO_2]/dt = CO_2 change per year, ppm in atm./year	a_1, positive, (Constant and independent of year) {2.082 ppm/year}	$2 * c_2 * year + c_1$ = {0.0378 * *year* + 1.473} {Fit 2.041 ppm/year with no. of years since 1991 = 15}
d[CO_2]/dt, CO_2 added to atm. GT in/year or required amount of CO_2 to be sequestered if *d[CO_2]/dt* needs to be zero.	$a_1 * 7.77$, (Constant and independent {16.2 GT of CO_2 added per year or 4.41 GT of C/year}	*{2 * c_2 * year + c_1} * 7.77 = {0.0378 * year + 1.473} * 7.77* {15.9 GT/year or 4.33 GT of C/year}
d[O_2]/dt = O_2 change per year, ppm in atm./year	b_1, negative, (Constant and independent of year {−4.438 ppm/year}	$2 * d_2 * years + d_1 = -0.0870 * \text{year} - 3.033_2 = -4.0438$ {−4.305 ppm/year}
d[O_2]/dt, Net O_2 removed from atm. In GT/year or required amount of O_2 to be added if d[$\lvert O_2 \rvert$]/dt in atm. Needs to be 0.	$\lvert b_1 \rvert * 5.65$, (Constant and independent {25.07 GT of O_2 depleted year}	*{2 * d_2 * year + d_1}* * 5.65 = $\lvert${0.0870 * year − 3.0332}$\rvert$ * 5.65* {24.3 GT/year}
$RQ_{Glob} = \left\{ \frac{d[CO_2]}{\lvert d[O_2]/dt \rvert} \right\}_{atm}$,	$\frac{a_1}{b_1}$, (Constant and independent of year) {$RQ_{G,\,lob}$ = 0.469}	$\left(\frac{2*c_2*year+c_1}{\lvert 2*d_2*year+\ d_1 \rvert} \right)$, decreases slightly with years, {RQ_{Glob} = 0.470}
Earth's annual mass loss rate due to *Net* C(s) mined, GT per year	$RQ_{Glob} * \lvert b1 \rvert * 0.177$, 1 or $a_1 * 2.12$, 4.43 GT/year}	$RQ_{Glob} * 0.177 * \lvert 2 * d_2 * year + d_1 \rvert$ Or $\lvert 2 * d_2 * year + d_1 \rvert * 2.12$, {4.334 GT/year}

For generating numbers for various parameters of interest listed in Table 2, the following data were used:

(a) $\dot{E}_{FFLU}$ = 460.21 in 2006 [73]. HHV_{O2} = 448 kJ/mole of O_2 = 0.448 * 10^{-3} Giga J/mole or 448 Exa J/Peta mole.
(b) For the year 2006, the oxygen consumption rate = 1.027 Peta mols/year with energy per year of 460.21 Exa J/year.
(c) RQ_{FF} = 0.75, RQ_{FFLU} = 0.775 with energy fraction from LU, EFLU = 0.11; $RQ_{LBM,}$ = 1, RQ_{OWBM} = 0.87, See also Ref. [77], which quotes PQ = 1.1 or RQ_{LBM} = 0.91 for terrestrial plants.

4. Results and Discussion

4.1. RQ of Fossil Fuels (FF)

As outlined in Section 3.4.1, the *RQ* was determined by two methods:

Method I. Figure 5 shows the results on fossil energy consumed (secondary *Y*-axis), Peta J/10, CO_2 in million tons/year (secondary *Y*-axis), and RQ_{FF} (primary *Y*-axis) vs. years (Equation (8)). It is seen that CO_2 produced by world-wide consumption of gas (*RQ* = 0.5), oil, and coal (*RQ* = 1) and energy released from all three sources of FF increased by almost 70%, while the RQ_{FF} estimated increases slightly with the years, indicating more use of coal. The average is about 0.75. The RQ_{FF} satisfies the inequality $0.5 < RQ_{FF} < 1$.

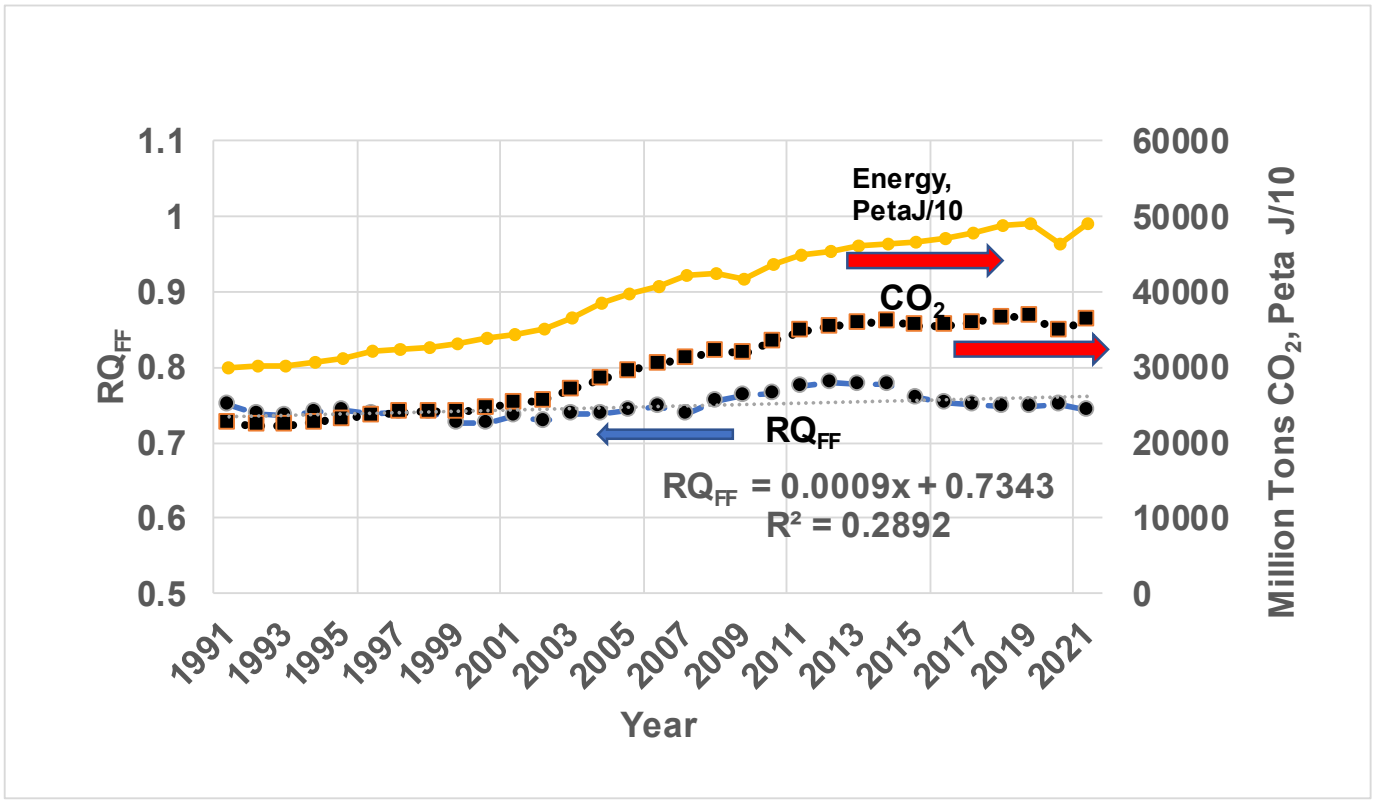

Figure 5. Variation of world fossil energy consumption in Peta J/10 (secondary axis, 1 Exa J = 1000 Peta J), CO_2 emission in million tons (secondary axis), and *RQ* of FF mix (RQ_{FF}, mix of gas, oil, and coal) in power plants (primary axis). "x" in Curve fit = (Year of interest-1991), Year of interest > 1991. The positive slope for RQ_{FF} indicates slightly increasing RQ indicating increased use of high RQ Fossil fuels. Note the low R^2. The source data for global CO_2 from both FF and LU, annual energy consumption by FF (gas, oil, and coal), and energy fractions by each type of FF are taken from Ref. [73]. In 1800, mostly biomass, a renewable fuel, was used. Thus, the only fossil fuel was coal, with $RQ_{Coal} = 1$ around 1800. For PNG and CSV data on FF, see Ref. [78], which also contains Keeling's curves. Also, this ref. [79] contains world energy data in addition to CO_2 and greenhouse gas emissions. With known CO_2 in GT/Exa J = 0.1 ∗ *RQ*, the RQ_{FF} ranges from 0.72 to 0.78 (a linear fit yields 0.73 + 0.0009 ∗ year) with an average of 0.75. Note: for natural gas, which is mostly methane, $RQ_{CH4} = 0.5$, while $RQ_{Coal} = 1$. Hence, 0.75 indicates *RQ* of a global average of fossil fuel mixtures of gas, oil, and coal [https://ourworldindata.org/grapher/global-primary-energy, accessed on 18 October 2022]. Ref. [80] states the average CO_2 emission from fossil energy from 2010–2019 is $35.2_{ig} \pm 1.8$ GT CO_2/year (9.6 ± 0.5 GT C/year) without the cement carbonation sink and 34.4 ± 1.8 GTt CO_2/year (9.4 ± 0.5 GTtC/year) with the cement carbonation sink. With this data, the average FF energy consumption is estimated at 450 Exa J.

Method II. Figure 6 shows a comparison of RQ_{FF} estimated using both Methods I and II. As before, RQ_{FF} estimated is slightly higher (1991–2009) but almost the same as the *RQ* from Method I for years beyond 2015.

4.2. RQ of FFLU {Combined FF and LU}

C emission data from FF and LU vs. year were collected along with energy released from FF, but land use energy data were not reported. Then, using C emission data for LU and assuming $RQ_{LU} \approx 1$, the land use energy was estimated by using Equation (8). With known total energy (FF + LU) in Exa J and known CO_2 in GT for both FF and LU, RQ_{FFLU} vs. year was estimated. Figure 7 shows the results. The RQ_{FFLU} average is about 0.78, which is slightly more than the RQ_{FF} due to the higher *RQ* of the land-use fuel source.

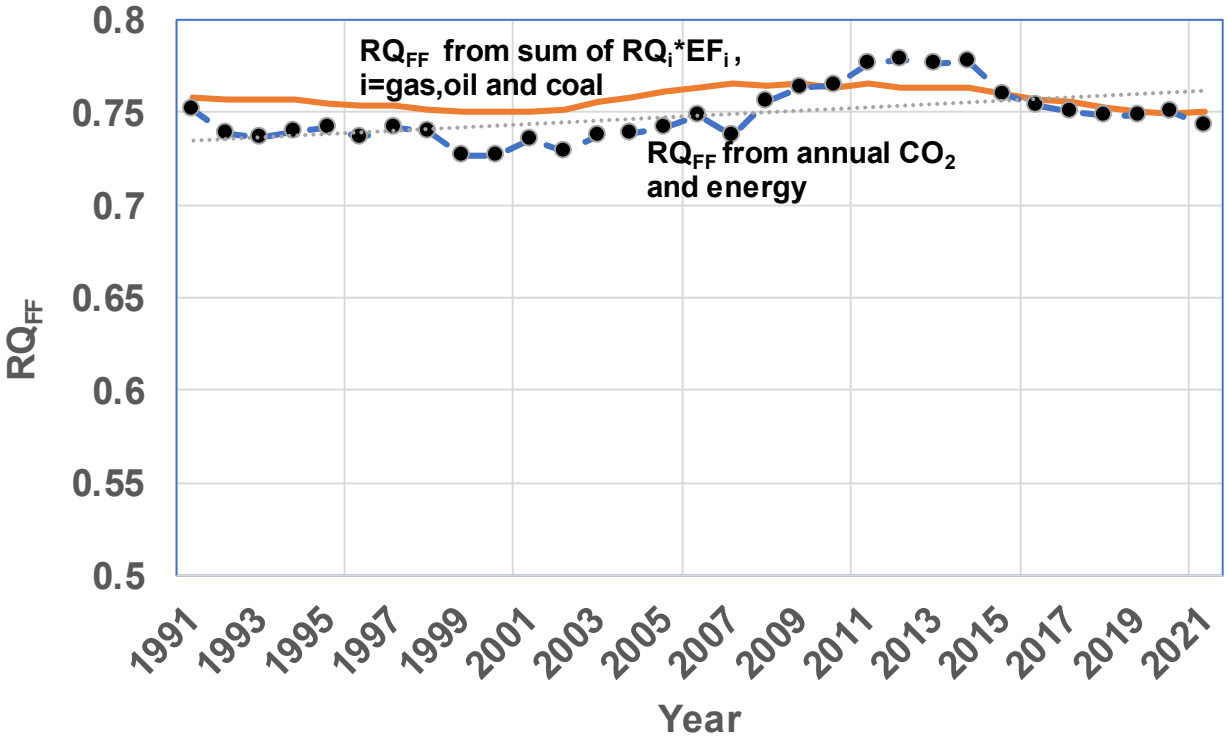

Figure 6. Comparison on Estimation of RQ_{FF} by Method I {reported CO_2 and energy data for land fuels used worldwide} with RQ_{FF} estimated using Method II {energy contributed and known RQ for each fuel type, {RQgas = 0.5, RQoil = 0.73, RQ Coal = 1}. Data are selected from Ref. [73]. Annual RQ_{FF} RQ varies depending on fuel mix used. EF is not shown for all years to reduce clusters of graphs. For 1990: EF_{gas} = 0.235, EF_{Oil} = 0.453, EF_{coal} = 0.312. EF in 2021: EF_{gas} = 0.297, EF_{Oil} = 0.376, EF_{coal} = 0.327. Both Methods I and II yield similar values for RQ_{FF}. Keeling presented the ExR (=1/RQ) as 1.4 or RQ_{FF} as 0.704–0.714 based on data around 1990 [55,81].

4.3. RQ of Land Biomass (RQ_{LBM}) and Ocean Water Based Biomass (RQ_{OWBM})

Appendix A.1 lists the ultimate analyses of several biomasses. Using the ultimate analysis, an empirical chemical formula was derived. For many biomass fuels listed in Ref. [82], Y_C (mass C sink in kg per kg of biomass) varies from 0.346 (rice straw) to 0.5441 (macadamia shells). See Appendix A.1 for the tabulation of RQ_{BM}. The RQ_{LBM} for land-based dry biomass ranges from 0.94 to 1.05 with an average of 1, which corresponds to a plant with UCF as CH_2O or a plant with pure C. It is noted that Huang et al. assumed RQ_{LBM} = 1, as though LBM has the chemical formula CH_2O [12]. Keeling quotes RQ_{LBM} = 0.95, which corresponds to the UCF, $CH_2O_{0.4}$ [55].

$$CO_2(g) + H_2O\ (l) \rightarrow CH_2O\ (s) + O_2\ (g),\ RQ_{LBM} = 1$$

4.4. Keeling's Data on CO_2 and O_2 in ppm and Curve Fits

4.4.1. Keeling's Data on CO_2 and O_2

The monthly data file presented by NOAA starting in 1990 was converted into Excel-based data. The calendar period since 1990 was first converted into days in order to capture the zigzag pattern by both CO_2 and O_2, and O_2 concentration in "per meg" units was converted into ppm basis, and the plot of CO_2 and O_2 vs. days/10 (Figure 8) reveals the zigzag pattern. Looking at the annual history of [CO_2] and [O_2] vs. year, it is clear that the concentration of CO_2 starts increasing while that of O_2 keeps decreasing from 1990 onwards. An explanation of the zigzag pattern is provided in Section 1 of the Introduction.

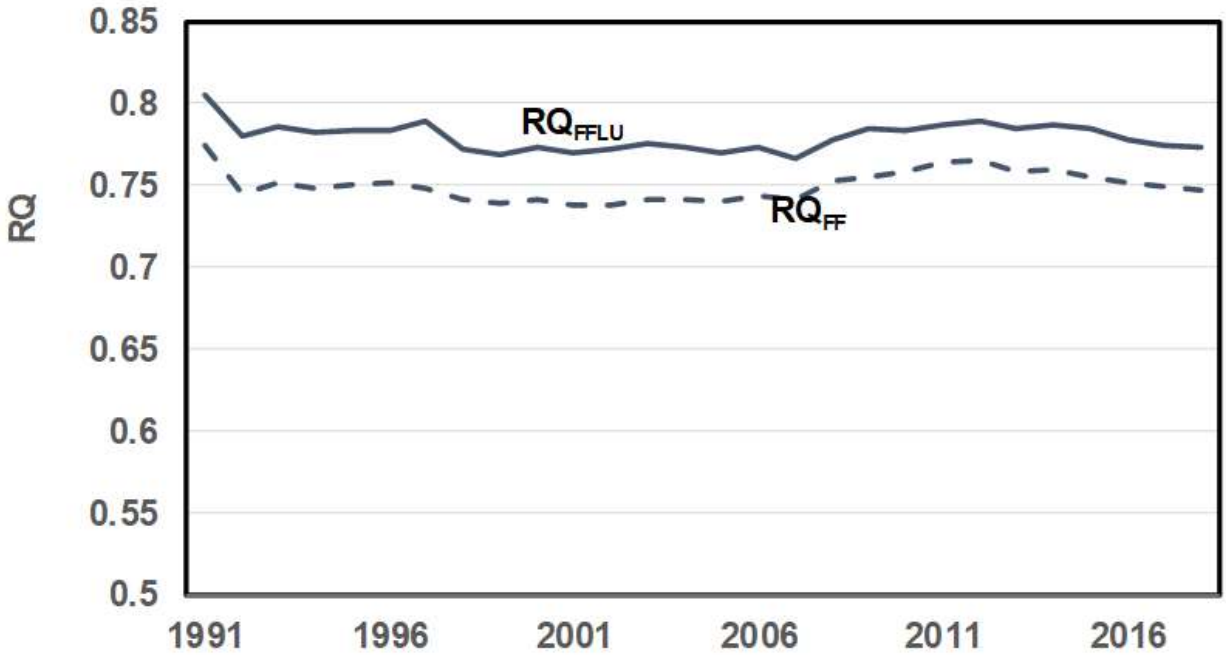

Figure 7. Comparison of *RQ* of FF and *RQ* of *RQ* combined FF and LU {RQ_{FFLU}}. Fossil energy data and fossil and land use C (thus CO_2) emission data are from Ref. [73]. Ref. [83] contains world energy data by oil, gas, and coal, 1800–2022. Land use includes CO_2 emitted via deforestation and CO_2 production via food and wood for construction. Land use CO_2 emissions are about 13–20% of total anthropogenic emissions [https://unfccc.int/topics/land-use/workstreams/land-use%E2%80%94land-use-change-and-forestry-lulucf, accessed on 3 November 2023]. Since land use CO_2 in GTt/Exa J = 0.1 $*$ RQ_{LU} *RQ* [7] and $RQ_{LU} \approx 1$ for LU this relation provides an estimate of energy released from land use data.

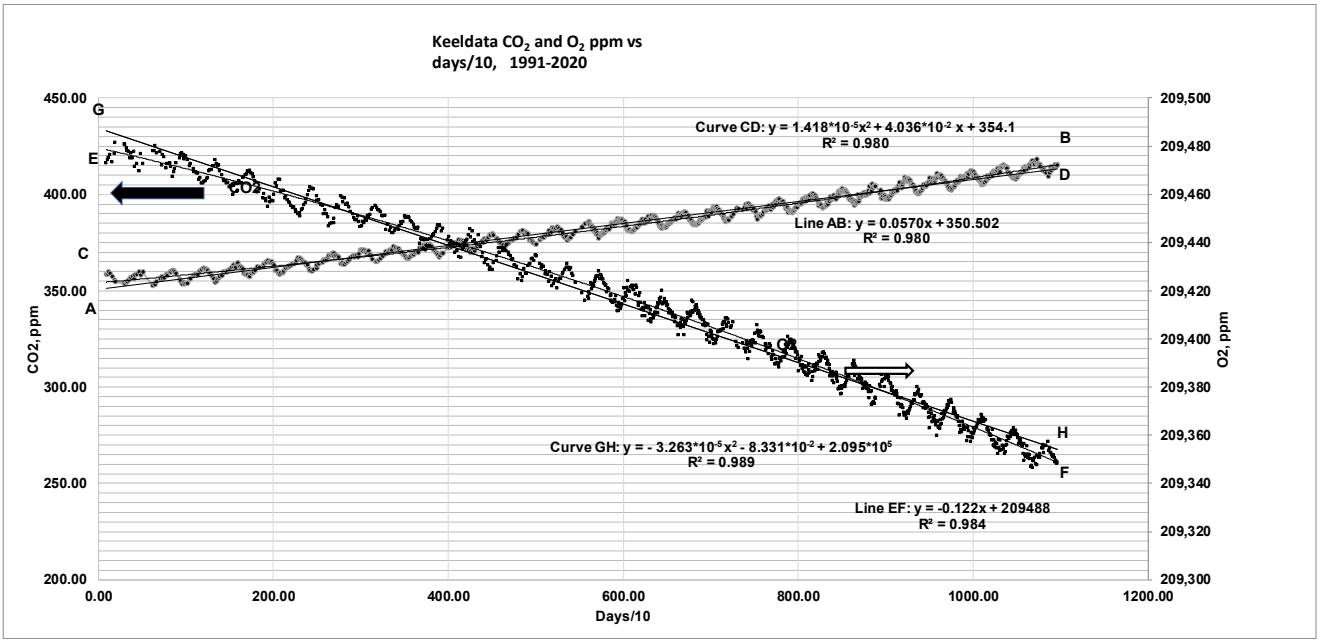

Figure 8. Keeling's data on CO_2 and O_2 and linear and quadratic fits based on data from 1991 to 2021. The Keeling data as Excel file can be accessed at the Scripps-CO_2 website [84]; also see Refs. [12,13]. The author converted the dates into days in order to capture saw tooth pattern. Day 1: 19 January 1991.

Apart from CO_2 released from power plants due to combustion of fuels [13] and CO_2 released from warmer oceans in SS, there are CO_2 sinks due to biomass growth in SS. For FW period ($CO_2 \uparrow$, $O_2 \downarrow$) due to the dominance of CO_2 added from power plants compared to CO_2 sink via biomass. Hence, there is seasonal "tap dance": $CO_2 \uparrow$, $O_2 \downarrow$ in FW while $CO_2 \downarrow$, $O_2 \uparrow$ in SS. Since the increase of CO_2 in FW > CO_2 sink in SS, the mean for CO_2 keeps increasing from year to year while the mean for O_2 decreases from year to year. In addition, planet earth is now constantly being charged with other pollutants, such as CH_4 with GWP = 10.4 (mole basis), 28.5 (mass basis), N_2O with GWP = 273 (mole or mass), and several other trace gases, essentially due to worldwide human activities. AB: straight line fit for CO_2, CD: quadratic fit for CO_2, EF: straight line fit for O_2, GH: quadratic fit for O_2. Ppm conversion to GT see ref [85].

4.4.2. The Curve Fits to Keeling's Data and Estimation of $d[CO_2]/dt$ and $d[O_2]/dt$

Two types of curve fits to Keeling data (from 18 April 1991 to 26 January 2021) on $[CO_2]$ and $[O_2]$ concentrations were obtained.

Linear Fit for CO_2 and O_2

If the fit is given in terms of (x' = days/10), say CO_2 in ppm = a_1 'x'+ $a_{0'}$ then the fit in terms of year is given as CO_2 in ppm = $a_{1'}$ year $*$ (365/10) + a_0. Let $a_1 = a_{1'} * (365/10)$, $a_{0'} = a_{0.}$ Thus, the trend line with a linear fit after conversion from days into years yields:

CO_2 in ppm = $a_1 *$ years+ a_0, a_1 = 2.0789, a_0 = 350.5 (linear fit), R_2 = 0.9709, linear, where years = Year of interest-1991, Year of interest $\geq$ 1991

In Column 3 of Table 2, the computed numbers for 2006 are given in parentheses in braces { } along with Keeling's data.

$$d[CO_2]/dt, \text{ ppm per year} = a_1 = 2.0789.$$

$$O_2 \text{ in ppm} = b_1 * \text{years+ } b_0,\ b_1 = -4.438 \text{ ppm/year},\ b_0 = 209{,}488 \text{ (linear fit)},\ R_2 = 0.9839$$

$$d[O_2]/dt \text{ ppm/per year} = b1 = -4.438 \text{ ppm per year}$$

Column 3 of Table 2 lists the linear curve fit constants along with corresponding derived formulae for several parameters of interest.

$$HHV_{O_2} = 448 \text{ kJ/mole} = 0.448 * 10^{-3} \text{ Giga J/mole or 448 Exa J/Peta mole}$$

4.4.3. Quadratic Fit for CO_2 and O_2 of Table 2

Since the atm contains air of mass of 5.13×10^{24} g or 1.77×10^6 Peta mol, 1 ppm change of any species by 1 ppm atm = 0.177 Peta mols and, as such, requires a large amount of change of species like CO_2 and O_2. More fossil fuel use results in more conversion of "carbon" from the ground to CO_2, more addition to the atmosphere, and more drop in O_2 concentration in the atmosphere, and thus slopes will become steeper in the future. Therefore, a linear fit is not reasonable, and the quadratic fit may reveal such an outcome.

Better accuracy is required, and hence the R^2 for the fit must be as high as possible. Thus, a quadratic fit was selected.

$$[CO_2] = CO_2 \text{ in ppm} = c_2 * years^2 + c_1 * years + c_0,\ c_2 = 0.01892,\ c_1 = 1.473,\ c_0 = 354.1,\ R^2 = 0.9804$$

$$\left\{\frac{d[CO_2]}{dt}\right\}_{atm} = 2 * c_2 * year + c_1 = 0.03784 * year + 1.473$$

where $\left\{\frac{d[CO_2]}{dt}\right\}_{atm}$ in ppm/year and

$$[O_2] = O_2 in\ ppm = d_2 * years^2 + d_1 * years + d_0,\ d_2 = -0.04347265,\ d_1 = -3.0332,\ d_0 = 209480,\ R^2 = 0.9896$$

$$\left\{\frac{d[O_2]}{dt}\right\}_{atm} = 2 * d_2 * year + d_1 = -0.0870 * year - 3.0332$$

where $\left\{\frac{d[O_2]}{dt}\right\}_{atm}$ in ppm/year. It is clear that R^2 is higher for a quadratic fit.

Column 3 of Table 2 summarizes coefficients fitted curves for both linear and quadratic fits. It also shows the comparison of results between curve fits and actual data. More is the energy consumption, more is the O_2 consumption and steeper the slopes of CO_2 and O_2 curves.

4.5. Estimation of Global Respiration Quotient (RQ_{Glob})

4.5.1. Global *RQ* Based on CO_2 Added to Atm and O_2 depleted from Atm

The global respiration coefficient is defined as

$$RQ_{Glob} = \frac{(d[CO_2]/dt)_{atm}}{|(d[O_2]/dt)_{atm}|} \quad (25)$$

where slopes are provided from curve fit constants on Keeling's curves.

Linear fit: The linear fit indicates that CO_2 increases by 2.09 ppm per year while atmospheric oxygen decreases at a rate of 4.438 ppm per year. Using a linear fit for Keeling's data on CO_2 and O_2 over 30 years (1991–2021) and Equation (24),

$$RQ_{Glob} = \frac{a_1}{b_1} = \frac{2.0789}{4.438} = 0.468, \ for\ linear\ fit \quad (26)$$

where "years" represents the (Year of interest—1991).

Quadratic Fit: Selecting a quadratic fit,

$$\frac{d[CO_2]}{dt} = 2 * c_2 * year + c_1 = 0.03784 * year + 1.473 \quad (27)$$

where $\frac{d[CO_2]}{dt}$ in ppm/year. Using Equation (24),

$$RQ_{Glob} = \left(\frac{2 * c_2 * years + c_1}{|2 * d_2 * years + d_1|}\right) = \frac{0.03784 * years + 1.473}{|-0.0435 * years - 3.0332|}, \ quadratic\ fit \quad (28)$$

See Column 3 of Table 2, Column 4 where results are tabulated for a quadratic fit. It is clear that *RQ* changes with the year. Columns 3 and 4 compare the results for linear and quadratic fits.

Figure 9 shows the variation of RQ_{Glob} with year based on a quadratic fit; it shows that RQ_{Glob} decreases from 0.48 to 0.46 while a linear fit yields a constant value of 0.47. The decrease in RQ_{Glob} is attributed to increasing CO_2 storage in the ocean. The RQ_{Glob} is not a property, while RQ_{FF} and RQ_{BM} are properties. The RQ_{Glob} is somewhat similar to the RQ_{vent} in biology. More detailed discussions are presented in the next section.

4.5.2. $RQ_{Glob} < RQ_{FFLU}$ and Physical Meaning of RQ_{Glob}

The $d[CO_2]/dt$ represents the net accumulation of CO_2 in atm. It is the difference between CO_2 added by FFLU and the sum of CO_2 sink by biomass and storage by oceans. Similarly, the magnitude of $\{d[O_2]/dt\}_{atm}$ represents the net depletion rate of O_2 in the atm. It is the difference between the O_2 used by FFLU and the O_2 produced by biomass.

The RQ_{Glob} depends on RQ_{FF}, RQ_{LBM}, RQ_{OWBM}, combined Land and ocean water biomass RQ_{LOWBM}, annual energy release, CO_2 sources, and CO_2 sinks. Expanding the relationship for RQ_{Glob},

$$RQ_{Glob} = \frac{\dot{N}_{CO_2,atm}}{\dot{N}_{O_2,atm}} = \frac{\dot{N}_{O_2,FFLU} * RQ_{FFLU} - \dot{N}_{O_2,LOWBM} RQ_{LOWBM} - \dot{N}_{CO_2,st,Ocn}}{\dot{N}_{O_2,FFLU} - \dot{N}_{O_2,LOWBM}} = \frac{RQ_{FFLU} - x * RQ_{LOWBM} - y}{(1-x)} \quad (29)$$

where $\dot{N}_{O_2,FFLU}$, O_2 consumed by FFLU, $x = \frac{\dot{N}_{O_2,LOWBM}}{\dot{N}_{O_2,FFLU}}$, $y = \frac{\dot{N}_{CO_2,st,Ocn}}{\dot{N}_{O_2,FFLU}}$, and $\dot{N}_{O_2,LOWBM}$ O_2 produced by both the land and ocean biomasses. Solutions for "x" and "y" are presented in Part II [86]. Since $RQ_{\text{FFLU}} = 0.78$ and $RQ_{\text{LOWBM}} \approx 1$ and approximating $RQ_{\text{FFLU}} \approx RQ_{\text{LOWBM}}$,

$$RQ_{Glob} \approx RQ_{FFLU} - \frac{y}{(1-x)} \quad (30)$$

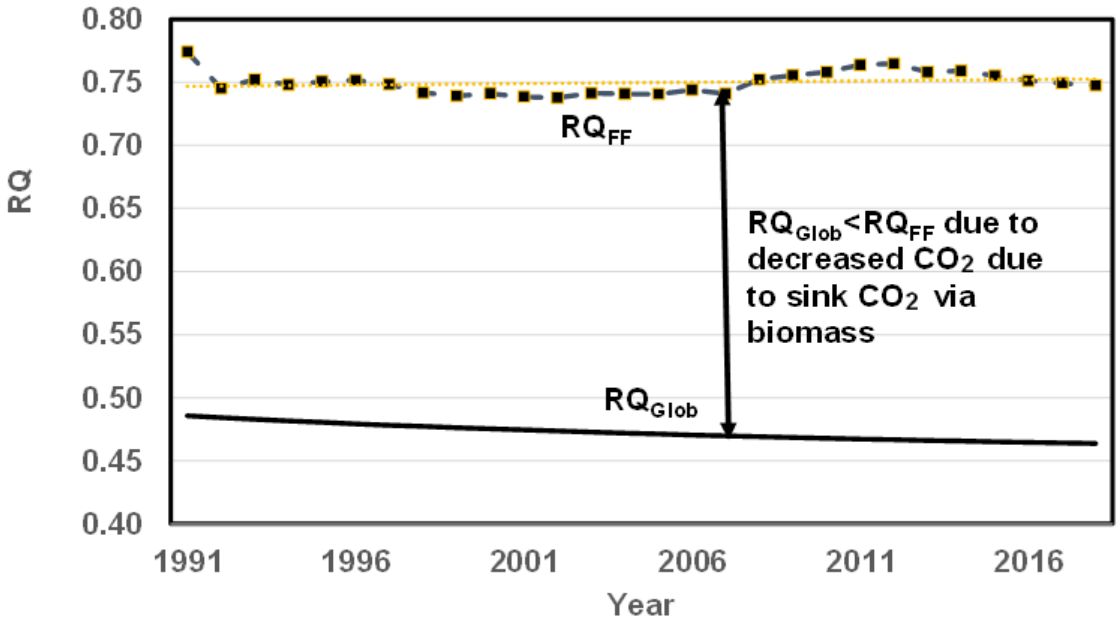

Figure 9. RQ_{Glob} (estimated from quadratic fit) and RQ_{FF} vs. year. There is a slight decrease in RQ_{Glob}. The lower the RQ_{Glob}, the lower the rate of increase in CO_2. $RQ_{\text{Glob}} < RQ_{\text{FFLU}}$ mostly due to the storage of CO_2 by oceans. Ideally, RQ_{Glob} should be zero so that the CO_2 concentration in the atm remains constant. Decreasing RQ_{Glob} is beneficial for planet earth since it indicates decreasing emissions of CO_2, but it is also an indication of increasing CO_2 storage in oceans.

It is apparent from Equation (30) that the greater the storage of CO_2 by the ocean {term: $y/(1-x)$}, the lesser is $RQ_{\text{Glob}} < RQ_{\text{FFLU}}$.

As an example, consider the year 2006, for which the annual energy release is known as 460 Exa J/year (which includes FF and LU). With constant HHV_{O2}, the O_2 consumed from the atm is given as 1.03 Peta mols/year and with $RQ_{\text{FFLU}} = 0.778$, the CO_2 released is $1.03 * 0.78 = 0.8$ Peta mols/year. The CO_2 added to the atm in ppm = 0.8/0.177 = 4.51 ppm since 1 ppm CO_2 added to the atm is equivalent to 0.177 Peta mols added to the atm. Similarly, O_2 removed from the atm in ppm = 1.03/0.177 = 5.8 ppm. If there were no biomass and no oceans, $RQ_{\text{Glob}} = RQ_{\text{FFLU}} = 0.778$. If the planet has only biomasses, they serve as CO_2 sinks and O_2 sources. Assuming % CO_2 sink by biomass to be 0.32 {Part II}, CO_2 sink by biomass = 1.46 ppm, and hence, net CO_2 added to the atm = 4.51 − 1.46 = 3.05 ppm. The O_2 added by biomass = 1.46 ppm. Thus, net O_2 removed from the atm is 5.8 − 1.46 = 4.34 ppm, assuming $RQ_{\text{LOWBM}} \approx 1$. Now RQ_{Glob} RQ = 3.05/4.34 = 0.7 and not much change from RQ_{FFLU} of 0.778. When ocean CO_2 storage of 23% of CO_2 from FFLU {Part II} is included, CO_2 as stored in the ocean = $0.23 * 4.51 = 1.04$ ppm, and hence, net CO_2 added to the atm = 3.05 − 1.04 = 2.01 ppm, close to Keeling's slope: d[CO_2]/dt = 2.02 ppm/year/ Now RQ_{Glob} = 2.01/4.34 = 0.46 ≈ 0.47< RQ_{FFLU}. Hence, the slope {d[CO_2[/dt}atm is affected more by the amount of CO_2 stored in oceans than by the extent of CO_2 sink by biomass. The higher the storage of CO_2 by oceans, the lower the RQ_{Glob} for given {d[O_2]/dt}atm and the higher the acidity of the ocean.

The RQ_{Glob} of 0.47 (<RQ_{FFLU} = 0.78) is interpreted as the global respiratory quotient of "hypothetical single fossil fuel (HSFF)" releasing 0.47 net moles of CO_2 {=CO_2 released from combustion of FFLU-CO_2 sink via BM and CO_2 storage in oceans} for every O_2 mole depleted (=O_2 consumed by FFLU-O_2 produced by LOWBM) from the atmosphere, as though this fictitious power plant is located on a barren earth without ocean water and chlorophyll on the planet. The number 0.47 multiplied by 12.01/44.01 = 0.273 indicates the net amount of moles of C depleted from the reserves of C on the planet. Figure 10 illustrates the difference between the green planet with oceans and the barren planet. Figure 10a represents the earth, with power plants burning FF or FFLU serving as a CO_2 source, biomasses undergoing PS with a CO_2 sink and O_2 source, and oceans serving as CO_2 storage. Figure 10b is a fictitious planet somewhat analogous to the metabolism in humans since the "fictitious" barren earth, without chlorophyll and oceans, does not have any mechanism to produce O_2 or provide a CO_2 sink.

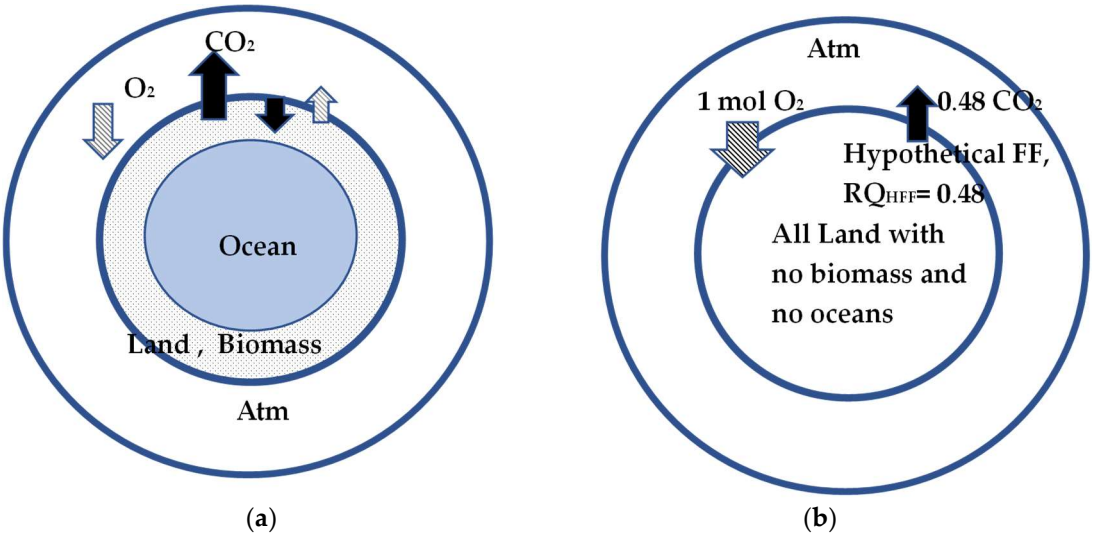

Figure 10. (**a**) Planet earth with biomass and oceans. The power plants add CO_2 and remove O_2 from the atm. PS of BM serves as a sink for a part of CO_2 emitted and replenishes the atm partly with O_2 produced by BM. (**b**) Barren planet earth without any biomass or oceans. For this planet, the RQ_{Glob} = 0.47. For each mole of O_2 depleted from the atm, 0.47 moles of CO_2 are added to atm. Hence, 0.47 moles of C or 5.84 kg of C is the mass difference between C of mined FF and the sum of C deposited for the growth of biomass on land and C(s) stored in oceans (which adds weight to land and oceans). Thus, net C(s) leaving land and converted to gaseous CO_2 decreases the weight of the earth.

Other consequences of Keeling's data and RQ_{Glob} are as follows: (i) Keeling's data indicate that the oxygen depletion rate in the atm is 4.48 ppm per year [Magnitude of slope of $\{d[O_2]/dt\}_{atm}$} and the CO_2 addition rate to the atm is 2.082 ppm/year [slope of $\{d\ [CO_2]/dt\}_{atm}$}. The normal atmospheric O_2 concentration in 1991 was 210,000 ppm. Thus, the depletion rate is extremely small compared to the initial oxygen concentration. However, it is well known that cells of BS do not receive oxygen when the O_2 % in atm falls below 16.5 16.5 % or 165,000 ppm [87]. Hence, O_2 will reach 165,000 ppm in about 12,000 years with linear fit of O_2 data (about 3000 years with quadratic fit) for human extinction or be depleted completely in about 47,000 {=210,000/4.48} years. (ii) The RQ_{Glob} of 0.47 indicates that 0.47 net moles of C were removed from the earth {C mined-C stored by ocean water-C removed biomass} and added to the atm as gaseous CO_2 per mole of O_2 depleted from the atm. Keeling's data indicate that with 4.3 ppm/year (Column 3 of Table 2) or 0.76 Peta mols of O_2/year, the annual loss of C(s) from earth is estimated as 4.3 GT, which presumes that (i) FF can be represented by C-H-O and no sequestration of CO_2. Alternately Keeling's data with linear fit indicates CO_2 gain tin atm to be 2.08 ppm

or Carbon converted into gas as $2.08 * 0.177 * 12.01 = 4.4$ GT/year (ii) All H in fuel gets converted into H_2O, which stays on the land/ocean. The C mass loss after 47000 years is estimated at 202,000 GT, {which includes C from coal, oil, and gas} or a decrease in earth's mass of 202,000 GT, which is negligible compared to the initial earth's mass of $5.97 * 10^{12}$ GT (iii) With CO_2 sequestration, the mass loss rate is almost zero. (iv) For the physiological effects of decreasing O_2 concentration, see Ref. [88]. (v) The atmospheric pressure is due to the weight of the air over the unit area. Once oxygen is depleted, the weight of the air column decreases, and hence, the atmospheric pressure will decrease due to the depletion of O_2. If CO_2 addition is ignored or sequestered using underground storage, the atmospheric pressure decreases to 79,000 Pa with 100% N_2 in the atmosphere. (vi) If CO_2 is not sequestered and continues to be at the current rate, it increases pressure above 79,000 Pa. Now the atm pressure is by both CO_2 and N_2, and it is estimated at 89,000 Pa {CO_2: 11% of N_2: 89%}. If all plants, trees, and PP cease to exist, the oxygen production stops [89] and if humans continue to use power plants, oxygen depletion rate due to FF will be 5.8 ppm per year and planet will run out of oxygen in 36,200 years !

4.5.3. RQ_{Glob} and Rationality for $RQ_{Glob} < RQ_{FF}$

RQ_{Glob} is around 0.48 in 1991 to and it decreases to 0.46 in 2021 when a quadratic fit is used (Figure 11) with an average of 0.47 and the RQ_{Glob} is constant at 0.47 with a linear fit.

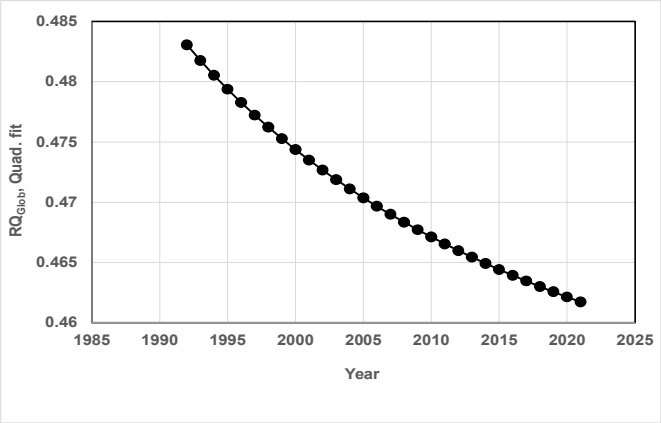

Figure 11. Variation of RQ_{Glob} since 1991 to 2021 for a quadratic fit of Keeling's data. The RQ_{Glob} decreases slightly from 0.48 in 1992 to 0.46 in 2021, revealing increasing acidity of the oceans. Part II of the manuscript indicates similar results. Note that the RQ_{Glob} RQ decreases increase in years for a quadratic fit but is constant for a linear fit.

Figure 11 shows decreasing RQ_{Glob} with a quadratic fit, revealing increased storage of CO_2 in oceans. Furthermore, the increasing ocean surface temperature may release O_2 into the atm, thus lowering the $RQ_{Glob.}$ [58]. It is seen from Equation (30) that increasing the storage of CO_2 in ocean water {term y, Equation (30)} lowers the RQ_{Glob}, which decreases the rate of increase of CO_2 in the atm, but at the cost of increasing the acidity of oceans. The website mentioned in Ref. [90] manages "ocean carbon and ocean acidification data", and the website confirms the increasing acidity of ocean water [91].

Unlike BS, which does not have any mechanism for O_2 production within the body, and hence, $0.7 < RQ < 1$ (without accounting for glycolysis), the breathing planet has a mechanism for O_2 production on land and OWBM. Ignoring $CO_{2,st,\,ocn,}$ the RQ_{Glob} is always less than RQ_{FFLU} for any $x < 1$. For a linear fit, the RQ_{Glob} is constant at $a_1/b_1 = 0.47$, but for a quadratic fit, RQ. Thus, the RQ_{Glob} average for 1991–2018 is about 0.47. Ideally, planet earth needs the RQ_{Glob} close to zero to maintain CO_2 at a constant value.

4.5.4. Predicted Saw-Tooth Pattern of O_2 Given CO_2 Data and RQ_{Glob}

Given the saw-tooth pattern of CO_2 data and RQ_{Glob} = 0.47, one can predict the O_2 pattern RQ (See Appendix A.2 ad Figure A1 for details). Suppose the first data i was on 19 January 1991 (day 1). Then there are a series of readings on several dates: 14 January 1991, 4 April 1991, 18 April 1991 . . . 18 April 1991 . . . 30 December 1994. The established O_2 in ppm (4 April 91) = O_2 in ppm (14 January 91), set at 209,474.2 ppm + {CO_2 data in ppm on 4 April 91- CO_2 in ppm 14 January 91}/RQ_{Glob}, estimated O_2 in ppm (18 April 91) = O_2 predicted (4 April 91) + {(CO_2 data in ppm on 18 April 91) − CO_2 in ppm 4 April 91)}/RQ_{Glob}, ... Figure 12 shows the saw-tooth pattern for CO_2 and O_2 (from data) and a comparison of data for O_2 with estimated O_2 using RQ_{Glob} for the period 1991–2020. Since distinction is not clear, Figure 13 shows the blown-up version of the comparison for a short period (1991–1994). It shows data on CO_2 and O_2 for 1992, 1993, and 1994, predicted O_2 (solid line) using R_{Glob} vs. days/10, where days are counted since 19 January 1991. Since the O_2 estimate uses CO_2 data, the estimated O_2 also reveals a saw-tooth pattern. The pattern and prediction of O_2 are explained as follows.

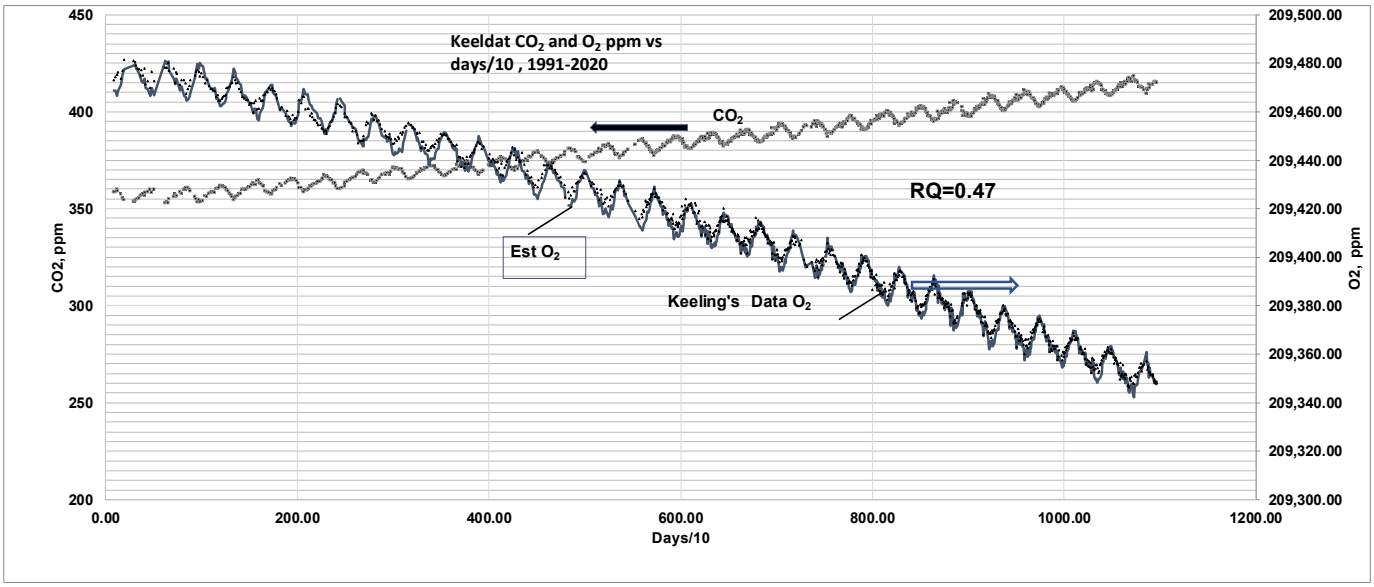

Figure 12. Comparison of saw-tooth patterns of CO_2 and O_2 with seasonal uptake of CO_2 by biomass in SS and FW. Given the saw-tooth pattern of CO_2 data (marker symbols), RQ_{Glob} = 0.47, O_2 concentrations are predicted as follows: The first data in 1991 were on 19 January 1991 (day 1). Then there are series of readings on 4 April 1991 (75 days from first reading), 18 April 1991 (89 days), 3 May 1991 (104 days), 16 May 1991 (117 days), 30 May 1991 (131 days), so on. . . Then predicted O_2, ppm (day 75) = O_2 in ppm (day 1) + {(CO_2 in ppm day 75) − CO_2 in ppm day 1)}/RQ_{Glob}, predicted O_2, ppm (day 89) = predicted O_2 in ppm (day 75) + {(CO_2 in ppm day 89) − CO_2 in ppm day 75)}/RQ_{Glob}, so on. The predicted saw-tooth pattern for O_2 in ppm (solid line) seems to match O_2 data (marker symbols) almost exactly for the scale selected. See Figure 13 for a blown-up version.

The solar input in FW is about 715 kWh/m^2 (over 6 months), while the input in SS is about 1130 kWh/m^2 (over 6 months), and hence, 57% more for solar input in SS compared to FW. Further, RQ_{SS} may be different compared to RQ_{FW}., i.e., the BM, a "mixture" of different types of trees and plants in SS and FW {e.g., live oak, which does not shed leaves, vs. post oak, which sheds leaves in FW), may be different in SS and FW, and as such, RQ's for BM may be different. Further, at the end of FW, the CO_2 may also be released by the oxidation of dead leaves by microbes, or the CO_2 sink in FW may be less compared to the CO_2 sink in SS. The O_2 production term due to biomass in Equation (29) for FW < O_2 production for SS. There is more depletion of O_2 in FW, and hence the slope of {d[O_2]/dt} in at $_{FW}$ in FW is also higher. Arguments could be repeated for SS, where CO_2 sink increases (numerator term in Equation (29)), lowering CO_2 in the atm by BM in SS. But it also

increases the O_2 production term in the denominator. Thus, compensating effects are present both in SS and FW, so RQ_{Glob} may be about the same in both FW and SS {see future work in the manuscript}, as the author assumed. But it is of concern whether the amplitude of variation in CO_2 by 6 ppm decreases with more annual energy consumption, which results in a higher release of CO_2 but not enough CO_2 sink in SS, thus decreasing the amplitude [92]. Keeling's data are for the northern hemisphere, and the data are not affected by the southern hemisphere (where the seasons are reversed) since the mixing time between the two hemispheres is of the order of one year [92].

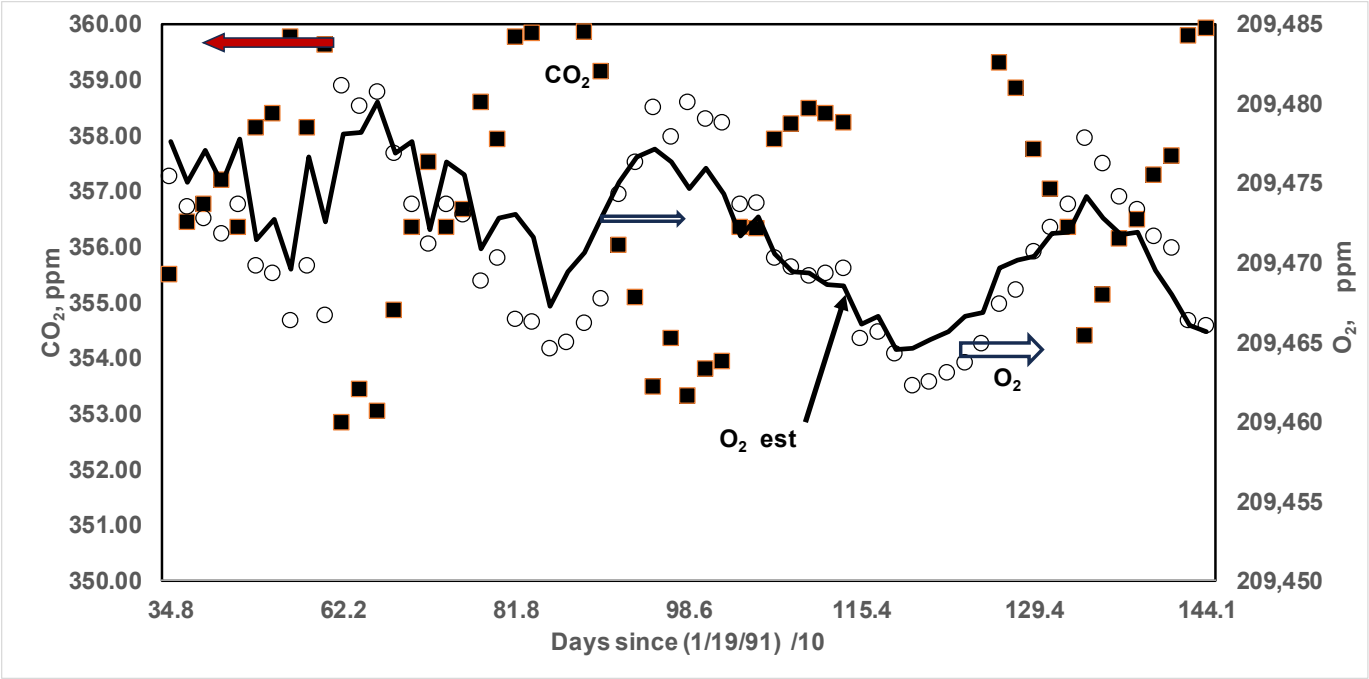

Figure 13. Magnified view of saw-tooth pattern for years 1991–1994 and comparison of predicted O_2. Solid symbols: CO_2 data, open symbol: O_2 data, solid line: O_2 computed using CO_2 data and constant $RQ = RQ_{SS} = RQ_{FW} = RQ_{Glob} = 0.47$ (see Appendix A.2 and Figure A1). The typical amplitude of CO_2 is approximately 6 ppm.

4.5.5. Death of BS vs. Death of Green Planet Earth

The BS can live when the *RQ* (0.7 to 1) and the oxidation reactions deliver the required energy for maintaining life-sustaining functions. However, those reactions involve electron transfer, resulting in the creation of a few radicals that cause damage to cells, thus resulting in the aging of the body and the eventual creation of a birth–death cycle. So, in order to live, the BS must eventually die. A faster oxidation reaction per unit mass of body (i.e., more energy release rate per unit mass, e.g., ants) results in a shorter life span [**65**]. Green planet earth consists of BS and NBS (e.g., sand, rocks, etc.) that breathe in oxygen and release CO_2 with an *RQ* of 0.47 to support mechanical and leisure life and to live comfortably. In doing so, the terrestrial system undergoes a self-destruction of ecosystems with increasing CO_2 in the atm, which results in global warming, the acidity of ocean water, and hence, the slow death of the green planet.

4.5.6. Earth Tilt Angle and Mining and Drilling of Fossil Fuels

The normal tilt angle of the earth is about 23.5 degrees. Earth has been shown to be tilted 80 cm (80 cm or 31.5") farther east over the last 30 years [93,94]. The tilt is attributed to pumping a large mass of water {2150 GT, 1993–2010 with a total of 17 years, 126 GT/year} from the reservoirs containing $2.0 * 10^{12}$ tons of water and a tilt of about 4.4 cm/year due to a shift in water masses. The tilt rate per unit mass of water shift is 0.037cm per GT. Similarly it was shown that mining fossil fuels at locations farther from axis of rotation

affects the mass distribution and can result in change in moment of inertia affecting earth's tilt; i.e., the tilt tangle is affected by pumping or, in general, removing a large amount of solid and liquid masses and converting them to gas and thus affecting mass distribution around the globe [94,95]. If so, then one could speculate that the tilt tangle may also be affected by pumping large amounts of oil and gas and mining coal out of the ground or, in general, removing a large amount of solid and liquid masses and converting them to gas and thus affecting mass distribution around the globe. Unlike the pumping of water, where water undergoes a cyclic process of pumping of water and recovery on land and ocean moderating tilt, the "pumping" of FF converts solids into gas in the atmosphere; as such, the problem of tilt may be more severe! In Section 4.5.2, it was determined that the C mass loss rate from the earth is 4.3 GT/year, and hence, for a period of 17 years, the total mass moved out is 73 GT. Apart from groundwater tilt, it is speculated that there could be an additional tilt of $73 * 0.037 = 2.7$ cm over 17 years!

4.5.7. Effects of Presence of CH_4 in the Atmosphere

In addition to CO_2 and CH_4, other global warming gases include H_2, N_2O, and SF_6. The CH_4 in the atm increases at a rate of 7.87 ppb/year (not shown) along with CO_2 at 2.08 ppm/year or a CO_2 total of $2.08 + 10 * 7.87/1000 = 2.16$ ppm/year. Note that the GWP of CH_4 is about 10 times that of CO_2. O_2 typically decreases at a rate of 4.44 ppm/year. Thus

$$RQ_{Glob,CO_2+CH_4} = \frac{\left(2.39 \text{ ppm} + 7.87\text{ppb} * 10^{-3}\left(\frac{\text{ppm}}{\text{ppb}}\right) * 10.4\right) * 10^{-6}\left(\frac{\text{moles}}{\text{ppm}}\right)}{4.44 \text{ ppm} * 10^{-6}\left(\frac{\text{moles}}{\text{ppm}}\right)} = 0.556, \text{GWPfor} CH_4 = 10.4 \quad (31)$$

Thus addition of CH_4, is equivalent to a total of 17 GT of CO_2 added to the atm.

4.5.8. RQ_{Glob} and CO_2 in Giga Tons per Exa J

When Equation (26) is used in Equations (8) and (9), *the relation does not yield GT per Exa J of energy release* but yields net GT of CO_2/year {i.e., CO_2 source—CO_2 sink via BM and storage} per Exa J of net energy release {=difference between the energy release from FFLU and energy input via solar energy during PS processes}. When the energy difference is divided by the average heating value of biomasses, it provides the mass of potential FF depleted from planet earth. Part II will introduce fossil energy-based $RQ_{Glob,En}$, which will provide CO_2 release per unit Exa J of energy release from FF so that a direct relation between annual FF energy and CO_2 in GT per Exa J can be provided.

5. Conclusions

The *RQ* concept borrowed from biology literature is adopted in engineering literature, and it provides a relation for CO_2 in GT per Exa J as $0.1 * RQ$ and CO_2 in million tons per MMBtu as equal to $0.116 * RQ$. For biomasses that serve as CO_2 sinks and O_2 sources, CO_2 sink in GT per Exa J energy input for biomass growth $= 0.1 * RQ$. Instead of *RQ*, the PS literature uses the following terms: *ExR*, RR, PQ, and RR which are equal to the inverse of *RQ*. Keeling's annual data on CO_2 and O_2 (1991–2018) are used to obtain the global *RQ* (RQ_{Glob}) as $RQ_{Glob} = 0.47$, which implies that net CO_2 moles added to the atm (after accounting for CO_2 sink by oceans and biomasses= 0.47 per unit) net mole of O_2 removed from the atmosphere *RQ*. The power plants on earth use natural gas ($RQ = 0.5$), oil ($RQ = 0.7$), and coal ($RQ = 1$) as FF. Based on CO_2 and the energy data, $RQ_{FF} \approx 0.78$. The global *RQ* for FF satisfies the inequality $0.5 < RQ < 1$. While RQ_{FF} or RQ_{BM} are properties of fuels and biomasses, RQ_{Glob} = is not a property and it depends on CO sink in atm, biomass and oceans. The global *RQ* is lower than 0.78 since the global *RQ* is affected by O_2 production and CO_2 sink in addition to CO_2 source and O_2 sink by FF, and hence the RQ_{Glob} of $0.47 < 0.78$. The FF with a lower *RQ* must be selected and biomass with high *RQ* is desired in order to reduce CO_2 added to the atmosphere. The saw-tooth pattern of O_2 is predicted with data on CO_2 and the global *RQ*.

6. Future Work

Future work must include the creation of genetically engineered biomasses with high *RQ* values greater than >1. The *RQ* concept, along with CO_2 and O_2 balance equations, may be used for estimating the CO_2 distribution in GTt/year and % distribution of CO_2 in the atm, land, and ocean, as well as storage in ocean water. The results must be validated by comparing the *RQ*-based results with those obtained from detailed computer models developed for CO_2 stored in the atm, land, and ocean water (Part II). Knowledge of the *RQ* for SS and FW is required in order to predict the saw-tooth patterns of CO_2 and O_2 concentrations. Data are needed for studying the effects of (a) oxygen depletion, (b) CO_2 addition, and (c) sequestration on the barometric pressure. Since water pumping seems to affect the earth's tilt angle [93], similar studies are needed on the effects of mining oil and solid fuels from the ground.

Supplementary Materials: The following supporting information can be downloaded at: https://www.mdpi.com/article/10.3390/en17020299/s1, Supplement on curve fits for Keeling's data on CO_2 and O_2.

Funding: The work was carried out simply because of curiosity generated by Keeling's data and its apparent link to *RQ* defined in biology. There was no funding for the current research on the *RQ* method for CO_2 distribution. The author wishes to acknowledge the partial support of the research funds from the Paul Pepper Professorship.

Data Availability Statement: Data are contained within the article and supplementary materials.

Acknowledgments: The author wished to acknowledge (i) Saravanan, Head Atm. Science Texas A&M for providing the author with a complimentary copy of his Book on "Climate Demon" Cambridge University Press, 2021) which contained Keeling's sawtooth curves on CO_2 and O_2, aroused the curiosity of author and provided the vital link to the *RQ* concept used in biology and engineering, (ii) Megan Simison of the J. Mike Walker '66 Department of Mechanical Engineering, Texas A&M University, for the English editing of the manuscript.

Conflicts of Interest: The author declares no conflict of interest.

Nomenclature

Atm	Atmosphere
BS	Biological system GPP: gross prod, total prod
C_{SI},C_{Eng}	See Section 3.3.2 on incomplete combustion/Flare
$\dot{C}$(s)	Carbon sink o source rate
CH	Carbohydrate
CO_2 eq	CO_2 equivalent
DAF	Dry ash free
$\dot{E}_{FFLU}$	Energy release rate from FFLU
EPICA	European Project for Ice Coring in Antarctica
ExR	Exchange ratio = 1/*RQ*
F	Fat
FF	Fossil fuel
FFLU	Fossil fuel and land use
FW	Fall or Autumn (Sep, Oct, Nov) and Winter (Dec, Jan, Feb)
GCB	Global Carbon Budget
GPP	Gross Primary Production
GWP	Global warming potential-CO_2 Equivalent
Giga J	10^9 J = 10^6 kilo J = 10^3 Mega J = 10^{-6} Peta J = 10^{-9} Exa J
GT	Giga tons, 10^9 Tons
HC	Hydrocarbon

HHV_{O_2}	Higher or gross heating value per Peta Oxygen moles
HSFF	Hypothetical Single Fossil Fuel
LBM	Land biomass
LOWBM	Combined land and ocean water biomasses
LU	Land use
M	Molecular weight
MOM	Marine organic matter
$\dot{N}_{CO_2}, \dot{N}_{O_2}$	Mole rates of CO_2, O_2 per year
$\dot{N}_{CO_2,FFLU}, \dot{N}_{O_2,FFLU}$	CO_2 release rate from FFLU and O_2 consumption by FFLU, Peta moles/year
NBS	Non-biological systems
$N_{C,nut}$	Number of C atoms in nutrient
$N_{CO_2,BM}$	number of moles of CO_2 used by biomass for growth
$N_{O_2,BM}$	number of moles of O_2 from biomass
NEP	Net Ecosystem Production
NPP	Net Primary Production, = GPP- respiration cost
Ocn	Ocean
OWBM	Ocean water biomass
NOAA	National Oceanic and Atmospheric Administration
NPP	Net Primary Product in ecosystem
Per meg	4.76 Per Meg = 1 ppm
PP	Phytoplankton
Ppb	Parts per billion
Ppm	Parts per million or molecules per million molecules 1 ppm in atm = 7.77 GT for CO_2, 2.12 GT for C, 1 ppm O_2 in atm = 5.65 GT [85]
PQ	Photosynthetic quotient {= $1/RQ$}
PS	Photosynthesis
Q	Heat
ρ	Density
RgQ	Regeneration Quotient (=$1/RQ$)
RQ	Respiratory Quotient, Subscript (i) BM Biomass, (ii) FF: Fossil Fuel (iii) FFLU: FF and land use, (iv) Glob: Global (v) Nut: nutrient, (vi) Vent: Ventilated
RR	Redfield ratio = $1/RQ$
SS	Spring (Mar, Apr, May) and Summer (June, July, Aug)
St	Storage
UCF	Unit Carbon Formula
$\dot{V}$	Volume flow rate
Y_k	Mass fraction of element k, g of k/g of mixture
z	Ratio of Oxygen moles supplied by ocean biomass to atm to total oxygen moles supplied by both Land and Ocean biomasses

Appendix A

There are two Appendices, with Appendix A listing RQ of land and a few oceans-based biomasses, and Appendix A.2 describes the method of obtaining saw-tooth patterns of O_2 from the data on CO_2.

Appendix A.1 Respiration Quotient (RQ) for Land Biomasses and Sea Weeds

Table A1. Respiration quotient (*RQ*) and C-Sink (g/g biomass) for Biomasses. Y_C, Carbon sink in g per g dry ash-free biomass, Boie Est (HHV, kJ/kg) = {35160 Y_C + 116225 ∗ Y_H − 11090 ∗ Y_O + 6280 Y_N + 10465 Y_S, where Y_C, Y_H, Y_N, Y_O, and Y_S are mass fractions of carbon, hydrogen, nitrogen, oxygen, and Sulphur in a C-H-N-O-S fuel. Table contains measured values of HHV. Min Y_C (g of C/g biomass): 0.346, Max Y_C: 0.544 Min *RQ* (mols CO_2 used/mols O_2 prod): 0.938, Max *RQ*: 1.046. Source data: [82,96].

Name	H/C	N/C	O/C	S/C	O/H	HHV, kJ/g	Y_C	Y_H	Y_N	Y_O	Y_S	*RQBM*
Field crops												
Alfalfa seed straw	1.373	0.0183	0.654	1.602×10^{-4}	0.476	18.45	0.468	0.054	0.01	0.407	0.0002	0.984
Bean straw	1.547	0.0166	0.785	8.718×10^{-5}	0.507	17.46	0.430	0.0559	0.0083	0.449	0.0001	1.006
Corn cobs	1.499	0.0086	0.733	8.042×10^{-5}	0.489	18.77	0.466	0.0587	0.0047	0.455	0.0001	0.992
Corn stover	1.515	0.0120	0.745	8.582×10^{-5}	0.492	17.65	0.437	0.0556	0.0061	0.433	0.0001	0.994
Cotton stalks	1.527	0.0261	0.744	1.898×10^{-4}	0.487	15.83	0.395	0.0507	0.012	0.391	0.0002	0.990
Rice straw (fall)	1.318	0.0144	0.657	7.173×10^{-4}	0.499	16.28	0.418	0.0463	0.007	0.366	0.0008	0.998
Rice straw (weathered)	1.351	0.0230	0.768	1.732×10^{-3}	0.568	14.56	0.346	0.0393	0.0093	0.354	0.0016	1.046
Wheat straw	1.376	0.0121	0.685	9.539×10^{-4}	0.497	17.51	0.432	0.05	0.0061	0.394	0.0011	0.997
Orchard prunings												
Almond prunings	1.226	0.0110	0.598	7.302×10^{-5}	0.488	20.01	0.513	0.0529	0.0066	0.409	0.0001	0.993
Black Walnut	1.390	0.0038	0.652	7.522×10^{-5}	0.469	19.83	0.498	0.0582	0.0022	0.433	0.0001	0.979
English Walnut	1.346	0.0064	0.651	7.534×10^{-5}	0.484	19.63	0.497	0.0563	0.0037	0.431	0.0001	0.989
Vineyard prunings												
Cabernet Sauvignon	1.493	0.0153	0.707	3.216×10^{-4}	0.474	19.03	0.466	0.0585	0.0083	0.439	0.0004	0.980
Chenin Blanc	1.459	0.0154	0.655	5.461×10^{-4}	0.449	19.13	0.480	0.0589	0.0086	0.419	0.0007	0.964
Pinot Noir	1.468	0.0156	0.685	7.947×10^{-5}	0.467	19.05	0.471	0.0582	0.0086	0.430	0.0001	0.976
Thompson seedless	1.449	0.0139	0.687	7.912×10^{-5}	0.474	19.35	0.474	0.0577	0.0077	0.433	0.0001	0.981
Tokay	1.449	0.0135	0.670	2.353×10^{-4}	0.462	19.31	0.478	0.0582	0.0075	0.426	0.0003	0.973
Energy crops												
Camaldulensis	1.425	0.0052	0.674	7.645×10^{-5}	0.473	19.42	0.490	0.0587	0.003	0.440	0.0001	0.981
Globulus	1.461	0.0069	0.688	7.775×10^{-5}	0.471	19.23	0.482	0.0592	0.0039	0.442	0.0001	0.979
Grandis	1.449	0.0027	0.701	7.751×10^{-5}	0.484	19.35	0.483	0.0589	0.0015	0.451	0.0001	0.988
Casuarina	1.426	0.0104	0.670	1.541×10^{-4}	0.469	19.44	0.486	0.0583	0.0059	0.434	0.0002	0.979
Cattails	1.452	0.0148	0.742	3.486×10^{-4}	0.511	17.81	0.430	0.0525	0.0074	0.425	0.0004	1.007
Popular	1.436	0.0083	0.677	7.732×10^{-5}	0.471	19.38	0.485	0.0585	0.0047	0.437	0.0001	0.980
Sudan grass	1.427	0.0233	0.660	6.722×10^{-4}	0.462	17.39	0.446	0.0535	0.0121	0.392	0.0008	0.973
Forest residue												
Black Locust	1.338	0.0096	0.620	7.384×10^{-5}	0.464	19.71	0.507	0.0571	0.0057	0.419	0.0001	0.976
Chaparral	1.288	0.0099	0.643	2.396×10^{-4}	0.499	18.61	0.469	0.0508	0.0054	0.402	0.0003	0.999
Madrone	1.476	0.0011	0.703	1.561×10^{-4}	0.476	19.41	0.480	0.0596	0.0006	0.450	0.0002	0.983
Manzanita	1.466	0.0030	0.696	1.555×10^{-4}	0.475	19.3	0.482	0.0594	0.0017	0.447	0.0002	0.982
Ponderosa Pine	1.446	0.0010	0.676	2.282×10^{-4}	0.467	20.02	0.493	0.0599	0.0006	0.444	0.0003	0.977

Table A1. *Cont.*

Name	H/C	N/C	O/C	S/C	O/H	HHV, kJ/g	Y_C	Y_H	Y_N	Y_O	Y_S	*RQBM*
Ten Oak	1.475	0.0022	0.693	7.835×10^{-5}	0.470	18.93	0.478	0.0593	0.0012	0.441	0.0001	0.978
Redwood	1.404	0.0008	0.636	2.219×10^{-4}	0.453	20.72	0.506	0.0598	0.0005	0.429	0.0003	0.968
White Fur	1.451	0.0009	0.686	7.645×10^{-5}	0.472	19.95	0.490	0.0598	0.0005	0.448	0.0001	0.980
Food and fiber processing wastes												
Almond hulls	1.392	0.0180	0.666	8.181×10^{-5}	0.478	18.22	0.458	0.0536	0.0096	0.406	0.0001	0.985
Almond shells	1.578	0.0221	0.705	1.666×10^{-4}	0.447	19.38	0.450	0.0597	0.0116	0.423	0.0002	0.960
Babassu husks	1.269	0.0044	0.631	2.978×10^{-4}	0.497	19.92	0.503	0.0537	0.0026	0.423	0.0004	0.998
Sugarcane bagasse	1.420	0.0073	0.663	8.362×10^{-5}	0.467	17.33	0.448	0.0535	0.0038	0.396	0.0001	0.977
Coconut fiber dust	1.194	0.0077	0.592	1.192×10^{-3}	0.495	20.05	0.503	0.0505	0.0045	0.396	0.0016	0.996
Cocoa hulls	1.289	0.0530	0.515	9.321×10^{-4}	0.399	19.04	0.482	0.0523	0.0298	0.331	0.0012	0.938
Cotton gin trash	1.580	0.0453	0.689	0	0.436	16.42	0.396	0.0526	0.0209	0.363	0	0.952
Macadamia shells	1.091	0.0057	0.548	6.885×10^{-5}	0.502	21.01	0.544	0.0499	0.0036	0.397	0.0001	1.001
Olive pits	1.518	0.0063	0.669	1.535×10^{-4}	0.441	21.39	0.488	0.0623	0.0036	0.435	0.0002	0.957
Peach pits	1.324	0.0052	0.554	3.534×10^{-4}	0.419	20.82	0.530	0.059	0.0032	0.391	0.0005	0.949
Peanut hulls	1.419	0.0305	0.649	9.822×10^{-4}	0.457	18.64	0.458	0.0546	0.0163	0.396	0.0012	0.970
Pistachio shells	1.440	0.0098	0.668	7.678×10^{-5}	0.464	19.26	0.488	0.0591	0.0056	0.434	0.0001	0.974
Rice hulls	1.248	0.0084	0.657	1.829×10^{-4}	0.526	16.14	0.410	0.043	0.004	0.359	0.0002	1.017
Walnut shells	1.359	0.0036	0.651	7.495×10^{-5}	0.479	20.18	0.500	0.0571	0.0021	0.434	0.0001	0.986
Wheat dust	1.466	0.0630	0.638	1.720×10^{-3}	0.436	16.2	0.414	0.051	0.0304	0.352	0.0019	0.953
Trees												
Maple wood (dry)	1.414	0.0042	0.619	0.000	0.438	16.2	0.506	0.0602	0.0025	0.417	0	0.958
Mesquite (as rec)	1.358	0.0122	0.578	2.578×10^{-4}	0.426	16.7	0.436	0.0498	0.0062	0.336	0.0003	0.952
Junifer (as rec)	1.370	0.0049	0.563	7.599×10^{-5}	0.411	19	0.493	0.0568	0.0028	0.370	0.0001	0.943
Sea Weeds [69]												
Sargassum tenerrimum	1.741	0.0248	1.420	1.809×10^{-2}	0.816	-	0.321	0.047	0.0093	0.607	0.0155	1.345
Sargassum sp. 1	1.593	0.0532	0.965	0.000	0.606	-	0.403	0.054	0.025	0.518	0	1.092
Sargassum sp. 2	1.777	0.0461	0.674	0.000	0.379	14.7	0.255	0.0381	0.0137	-	0	0.903
Sargassum horneri	1.512	0.0161	0.647	1.355×10^{-2}	0.428	15.44	0.489	0.0622	0.0092	0.422	0.0177	0.936
Sargassum fluitans Dirty	1.629	0.0460	0.725	1.442×10^{-2}	0.445	13.87	0.270	0.037	0.0145	0.261	0.0104	0.944
Sargassum fluitans Wash	1.523	0.0362	0.706	7.579×10^{-3}	0.464	15.27	0.391	0.05	0.0165	0.367	0.0079	0.966
OTHERS	0.000	0.0000	0.000	0.000	0.000	0	0.000	0	0	0.000	0	0.000
Pineapple	1.898	0.0171	0.799	0.000	0.421	15.27	0.401	0.064	0.008	0.427	0	0.930
Grass	1.585	0.0190	0.717	8.325×10^{-4}	0.452	15.27	0.450	0.06	0.01	0.430	0.001	0.963

In terms of energy units, the total annual primary biomass production on earth (including food, fiber, etc.) is estimated at 1260 EJ/year [97]. Note that the term biomass includes both land- and water-based. Assuming that the biomass is not in oxidized form, the O_2 added to the atm through PS is 2.8 Peta moles, assuming the energy required per mole of O_2 is the same as the higher heating value per mole of O_2, $\{HHV_{O_2}\}$ = 448 Exa J/Peta mole of O_2 [6,7]. For different sea weeds, ref. [69] presents ultimate analyses; the author determined all of the empirical chemical formulae. Also, Sargassum for Sp 1 and Sp 2 assumes $Y_S = 0$; further, for Sp. 2, Y_O is assumed to be equal to $1\text{-}Y_C\text{-}Y_H\text{-}Y_N$

Appendix A.2 Saw Tooth Pattern Using RQ_{Glob}

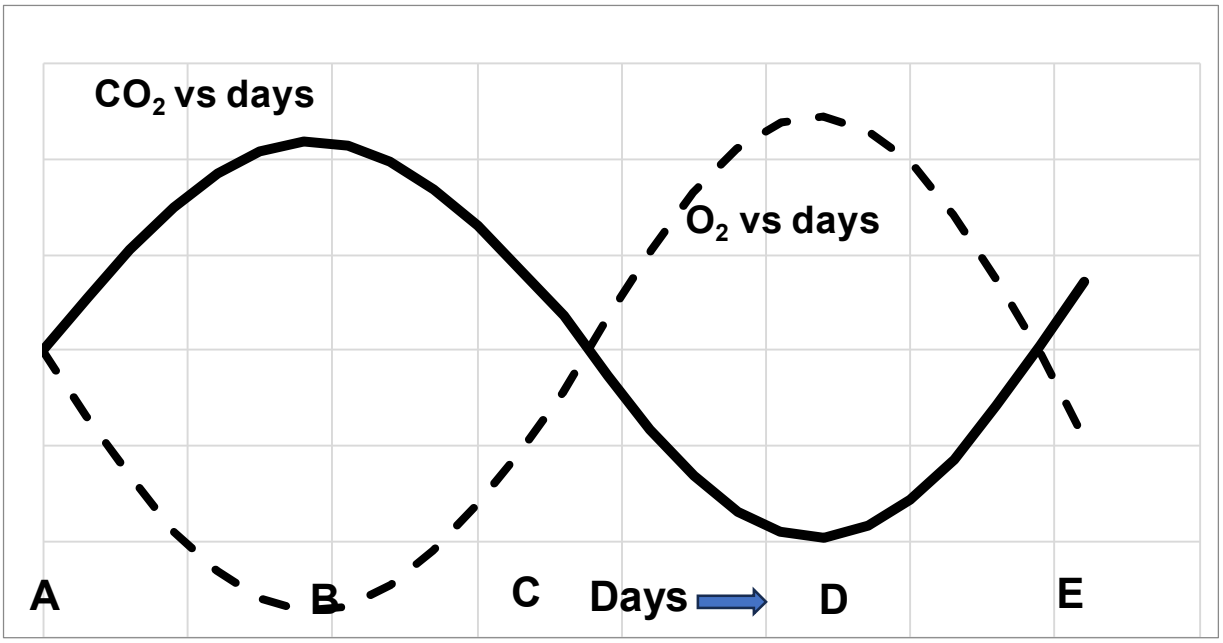

Figure A1. Schematic of CO_2 and O_2 vs. days. Data for CO_2 are available on days A, B, C, D, and E. O_2 vs. Days are generated using CO_2 data and *RQ* for SS and FW. AB, CD: FW, BC, DE: SS, Typically CO_2, at C > CO_2 at A and O_2 at C < O_2 at A.

Refer to Figure A1. The relation between oxygen concentration at B in terms of oxygen concentration at A, RQ_{Glob}, and CO_2 concentrations at A and B is given as follows:

$$[O_{2,B}\ ] = [O_{2,A}] - ([CO_{2,B}] - [CO_{2,A}])/RQ_{FW} \quad \text{(A1)}$$

Similarly, O_2 at C is given as

$$[O_{2,C}] = [O_{2,B}] + ([CO_{2,B}] - [CO_{2,c}])/RQ_{SS} \quad \text{(A2)}$$

where [ ] concentrations in ppm. Using Equation (A1),

$$[O_{2,C}] = [O_{2,A}] - ([CO_{2,B}] - [CO_{2,A}])/RQ_{FW} + ([CO_{2,B}] - [CO_{2,c}]/RQ_{SS} \quad \text{(A3)}$$

Simplifying and rearranging,

$$[O_{2,C}] - [O_{2,A}] = [CO_{2,B}]\left(\frac{1}{RQ_{SS}} - \frac{1}{RQ_{FW}}\right) + \frac{[CO_{2,A}]}{RQ_{FW}} - \frac{[CO_{2,C}]}{RQ_{SS}} \quad \text{(A4)}$$

The first term on the right is positive. Furthermore, $CO_{2,C} > CO_{2,A}$. The second term on the right within { } is positive. Hence $[O_{2,C}] < [O_{2,A}]$ In FW, solar energy input is less for PS, while input energy is higher in SS. Hence, there is rapid biomass growth in SS compared to FW, and as such, the CO_2 sink is higher in SS compared to FW. Thus, RQ_{BM}

in FW may not be the same as RQ_{SS}. *RQ* for BM is a mixture of *RQ*'s of various types of plants whose *RQ*'s may differ.

$$RQ_{\text{Glob}} = \text{CO}_2 \text{ added to atm}/\text{O}_2 \text{ depleted from atm}$$

The CO_2 sink in FW may be less compared to the CO_2 sink in SS, thus increasing CO_2 with a higher value for $(a_1)_{FW}$. At the same time, O_2 production in FW < O_2 production in SS, thus depleting more O_2 in FW, and hence $|b_{1|FW}$ is also higher. Arguments could be repeated for SS, where CO_2 sink increases, lowering $\{a_1\}_{SS}$ along with a decrease in $|b_1|SS$. i.e., compensating effects are present both in FW and SS, and hence one may assume that RQ_{Glob} remains approximately constant.

Assuming $RQ_{SS} = RQ_{FW} = RQ_{Glob}$, then after simplification, Equation (A4) becomes

$$[O_{2,C}] - [O_{2,A}] = \left(\frac{[CO_{2,A}] - [CO_{2,C}]}{RQ_{Glob}} \right) \tag{A5}$$

where typically $[CO_{2,C}] > [CO_{2,A}] - Thus\ [O_{2,C}] < [O_{2,A}]$.

$$RQ_{Glob} = \left(\frac{[CO_{2,C}] - [CO_{2,A}]}{|[O_{2,C}] - [O_{2,A}]|} \right) \approx \left(\frac{\left\{ \frac{d[CO_2]}{dt} \right\}_{atm}}{\left| \frac{d[O_2]}{dt} \right|_{atm}} \right), Keeling\ Curves \tag{A6}$$

References

1. Available online: https://www.biologyonline.com/dictionary/life (accessed on 8 September 2022).
2. Available online: https://www.cropnutrition.com/nutrient-knowledge/oxygen (accessed on 22 December 2021).
3. Available online: https://greencover.com/category/seed-production/ (accessed on 8 November 2022).
4. Available online: https://archive.ipcc.ch/ipccreports/sres/land_use/index.php?idp=24 (accessed on 24 October 2023).
5. Boden, T.A.; Marland, G.; Andres, R.J. Global, Regional, and National Fossil-Fuel CO_2 Emissions. In *Carbon Dioxide Information Analysis Center, Oak Ridge National Laboratory*; U.S. Department of Energy: Oak Ridge, TN, USA, 2010.
6. Annamalai, K. Respiratory quotient (*RQ*), exhaust gas analyses, CO_2 Emission and applications in automobile engineering. *Adv. Automob. Eng.* **2013**, *2*, 2–4. [CrossRef]
7. Annamalai, K.; Thanapal, S.; Ranjan, D. Ranking renewable and fossil fuels on global warming potential using respiratory quotient (*RQ*) Concept. *J. Combust.* **2018**, *2018*, 1270708. [CrossRef]
8. Hansen, J.; Sato, M.; Ruedy, R.; Lacis, A.; Oinas, V. Global warming in the twenty-first century: An alternative scenario. *Proc. Natl. Acad. Sci. USA* **2000**, *97*, 9875–9880. [CrossRef] [PubMed]
9. Crutzen, P.J.; Mosier, A.R.; Smith, K.A.; Winiwarter, W. N_2O release from agro-biofuel production negates global warming reduction by replacing fossil fuels. *Atmos. Chem. Phys. Discuss.* **2007**, *7*, 11191–11205.
10. Hotsmark, B. Quantifying the global warming potential of CO_2 emissions from wood fuels. *Glob. Energy* **2015**, *7*, 195–206.
11. Nejat, P.; Jomehzadeh, F.; Taheri, M.M.; Gohari, M.; Majid, M.Z.A. A global review of energy consumption, CO_2 emissions and policy in the residential sector (with an overview of the top ten CO_2 emitting countries). *Renew. Sustain. Energy Rev.* **2015**, *43*, 843–862. [CrossRef]
12. Keeling, C.D.; Piper, S.C.; Bacastow, R.B.; Wahlen, M.; Whorf, T.P.; Heimann, M.; Meijer, H.A. Atmospheric CO_2 and $13CO_2$ Exchange with the Terrestrial Biosphere and Oceans from 1978 to 2000: Observations and Carbon Cycle Implications. In *A History of Atmospheric CO_2 and Its Effects on Plants, Animals, and Ecosystems*; Ecological Studies; Springer: New York, NY, USA, 2005; Volume 177, pp. 83–113.
13. Saravanan, R. *Climate Demon*; Cambridge Univ Press: Cambridge, UK, 2021.
14. Balkanski, Y.; Monfray, P.; Battle, M.; Heimann, M. Ocean primary production derived from satellite data: An evaluation with atmospheric oxygen measurements. *Glob. Biogeochem. Cycles* **1999**, *13*, 257–271. [CrossRef]
15. Available online: https://askdruniverse.wsu.edu/2020/01/10/trees-create-oxygen/ (accessed on 16 October 2022).
16. Keeling, R.F. *Scripps O_2 Program Data*; UC San Diego Library Digital Collections: San Diego, CA, USA, 2019. [CrossRef]
17. Huang, J.; Huang, J.; Liu, X.; Li, C.; Ding, L.; Yu, H. The global oxygen budget and its future projection. *Sci. Bull.* **2018**, *63*, 1180. [CrossRef]
18. Available online: https://scripps.ucsd.edu/news/broken-record-atmospheric-carbon-dioxide-levels-jump-again#:~:text=Scripps%20recorded%20a%20May%20CO,an%20elevation%20of%2013,600%20feet (accessed on 14 October 2023).
19. Duursma, E.K.; Boission, M.P.R.M. Global oceanic and atmospheric oxygen stability considered in relation to the carbon cycle and to different time scales. *Oceanol. Acta* **1994**, *17*, 117–141.
20. Duffy, K.A.; Schwalm, C.R.; Arcus, V.L.; Koch, G.W.; Liang, L.L.; Schipper, L.A. How close are we to the temperature tipping point of the terrestrial biosphere? *Sci. Adv.* **2021**, *7*, 3. [CrossRef]

21. Available online: https://www.chegg.com/homework-help/questions-and-answers/data-let-s-use-1951-1980-average-global-temperature-14-c-base-temperature-create-new-colum-q34424338 (accessed on 24 October 2023).
22. Jouzel, J.; Masson-Delmotte, V. EPICA Dome C Ice Core 800KYr deuterium data and temperature estimates. *Pangaea* **2007**. [CrossRef]
23. Lüthi, D.; Le Floch, M.; Bereiter, B.; Blunier, T.; Barnola, J.-M.; Siegenthaler, U.; Raynaud, D.; Jouzel, J.; Fischer, H.; Kawamura, K. High-resolution carbon dioxide concentration record 650,000–800,000 years before present. *Nature* **2008**, *453*, 379–382. [CrossRef] [PubMed]
24. Jouzel, J.; Masson-Delmotte, V.; Cattani, O.; Dreyfus, G.; Falourd, S.; Hoffmann, G.; Minster, B.; Nouet, J.; Barnola, J.M.; Chappellaz, J.; et al. Orbital and millennial Antarctic climate variability over the past 800,000 years. *Science* **2007**, *317*, 793–797. [CrossRef] [PubMed]
25. Available online: https://eng.libretexts.org/Bookshelves/Environmental_Engineering_(Sustainability_and_Conservation)/Energy_Conservation_for_Environmental_Protection_(Pisupati) (accessed on 24 October 2023).
26. Available online: https://www.saildrone.com/news/hurricane-sam-saildrone-sails-back-into-eye-storm (accessed on 24 October 2023).
27. Available online: https://www.nytimes.com/interactive/2023/05/09/magazine/hurricane-saildrone.html?unlocked_article_code=VUzdTI4_2Wkbe3pfTGzCSB6C-YwQ-xsFx00o1N8VWsm9ruYqPH8NHVCHj7epbQZdWW5v_5AfzFD3A-GAeKfNoskNsNxBqdlL8EnPCOqk7lhC3wec5TfyBq0X_-hXbKz4fvsT-B (accessed on 9 May 2023).
28. Available online: https://urldefense.com/v3/__https://www.weather.gov/media/slc/ClimateBook/Annual*20Average*20Temperature*20By*20Year.pdf__;JSUlJQ!!KwNVnqRv!EkkZzI7LzrTnM3yjfkgKjKtJtqVJ9HO57RQ3sIC32HeaVd51lXEd0bjoolC_4xrzE98kvNco2hXO6U33z4lgxFAy5A$ (accessed on 10 May 2023).
29. Zhu, Q.; Jiang, H.; Liu, J.; Peng, C.; Fang, X.; Yu, S.; Zhou, G.; Wei, X.; Ju, W. Forecasting carbon budget under climate change and CO_2 fertilization for subtropical region in China using integrated biosphere simulator (IBIS) model. *Pol. J. Ecol.* **2011**, *59*, 3–24. Available online: https://pubs.usgs.gov/publication/70036163 (accessed on 10 May 2023).
30. Friedlingstein, P.; O'Sullivan, M.; Jones, M.W.; Andrew, R.M.; Gregor, L.; Hauck, J.; Le Quéré, C.; Luijkx, I.T.; Olsen, A.; Peters, G.P.; et al. Global Carbon Budget 2022. *Earth Syst. Sci. Data* **2022**, *14*, 4811–4900. [CrossRef]
31. Gasser, T.; Crepin, L.; Quilcaille, Y.; Houghton, R.A.; Ciais, P.; Obersteiner, M. Historical CO_2 emissions from land use and land cover change and their uncertainty. *J. Biogeosci.* **2020**, *17*, 4075–4101. [CrossRef]
32. Watson, R.T.; Noble, J.R.; Bolin, B.; Ravindranath, N.H.; Verardo, D.J.; Dokken, D.J. (Eds.) *Land Use, Land-Use Change and Forestry*; IPCC: Geneva, Switzerland; Cambridge University Press: Cambridge, UK, 2000.
33. Gloege, L.; Yan, M.; Zheng, T.; McKinley, G.A. Improved quantification of ocean carbon uptake by using machine learning to merge global models and pCO_2 data. *J. Adv. Model. Earth Syst.* **2022**, *14*, e2021MS002620. [CrossRef]
34. Terhaar, J.; Frölicher, T.L.; Joos, F. Observation-constrained estimates of the global ocean carbon sink from Earth system models. *J. Biogeosci.* **2022**, *19*, 4431–4457. [CrossRef]
35. Li, H.; Ilyina, T.; Loughran, T.; Spring, A.; Pongratz, J. Reconstructions and predictions of the global carbon budget with an emission-driven Earth system model. *Earth Syst. Dyn.* **2023**, *14*, 101–119. [CrossRef]
36. Yakir, D. Large rise in carbon uptake by land plants. *Nature* **2017**, *544*, 39–40. [CrossRef]
37. David, K. Expected Limits on the Potential for Carbon Dioxide Removal from Artificial Upwelling. *J. Front. Mar. Sci.* **2022**, *9*, 841894. [CrossRef]
38. Li, C.; Huang, J.; Ding, L.; Liu, X.; Han, D.; Huang, J. Estimation of Oceanic and Land Carbon Sinks Based on the Most Recent Oxygen Budget. *Earth's Fut.* **2021**, *9*, e2021EF002124. [CrossRef]
39. Matthews, H.D.; Zickfeld, K.; Knutti, R.; Allen, M.R. Focus on cumulative emissions, global carbon budgets and the implications for climate mitigation targets. *Environ. Res. Lett.* **2018**, *13*, 010201. [CrossRef]
40. Available online: https://github.com/openclimatedata/global-carbon-budget/blob/main/data/global-carbon-budget.csv#L2 (accessed on 9 May 2023).
41. Available online: https://spacemath.gsfc.nasa.gov/earth/6Page54.pdf (accessed on 9 November 2023).
42. Moreno, A.R.; Garcia, C.A.; Larkin, A.A.; Lee, J.A.; Wang, W.L.; Moore, J.K.; Primeau, F.W.; Martiny, A.C. Latitudinal gradient in the respiration quotient and the implications for ocean oxygen availability. *Proc. Natl. Acad. Sci. USA* **2020**, *117*, 22866–22872. [CrossRef] [PubMed]
43. Redfield, A.C.; Ketchum, B.H.; Richards, F.A. The influence of organisms on the composition of seawater. *Sea* **1963**, *2*, 26–77.
44. Silva, C.; Annamalai, K. Entropy Generation and Human Aging: Lifespan Entropy and Effect of Physical Activity Level. *J. Entropy* **2008**, *10*, 100–123. [CrossRef]
45. Annamalai, K.; Puri, I.K.; Jog, M.A. *Advanced Thermo-Dynamics Engineering*, 2nd ed.; CRC/Taylor and Francis: Boca Raton, FL, USA, 2011.
46. Al-Saady, N.M.; Blackmore, C.M.; Bennett, E.D. High fat, low carbohydrate, enteral feeding lowers $PaCO_2$ and reduces the period of ventilation in artificially ventilated patients. *Intensive Care Med.* **1989**, *15*, 290–295. [CrossRef]
47. Available online: https://en.wikipedia.org/wiki/Respiratory_quotient (accessed on 11 October 2023).
48. Available online: https://www.frontiersin.org/articles/10.3389/fendo.2018.00806/full (accessed on 11 October 2023).
49. Available online: https://www.lung.org/lung-health-diseases/lung-disease-lookup/copd/living-with-copd/nutrition (accessed on 11 October 2023).

50. Pujia, A.; Mazza, E.; Ferro, Y.; Gazzaruso, C.; Coppola, A.; Doldo, P.; Grembiale, R.D.; Pujia, R.; Romeo, S.; Montalcini, T. Lipid Oxidation Assessed by Indirect Calorimetry Predicts Metabolic Syndrome and Type 2 Diabetes. *Front. Endocrinol.* **2018**, *9*, 806. [CrossRef]
51. Patel, H.; Kerndt, C.C.; Bhardwaj, A. *Physiology, Respiratory Quotient*; StatPearls Publishing: Treasure Island, FL, USA, 2023. Available online: https://www.ncbi.nlm.nih.gov/books/NBK531494 (accessed on 24 August 2023).
52. Available online: https://en.wikipedia.org/wiki/Composition_of_the_human_body (accessed on 19 August 2023).
53. Anderson, L.A. On the hydrogen and oxygen content of marine phytoplankton. *Deep-Sea Res.* **1995**, *42*, 1675–1680. [CrossRef]
54. Available online: https://en.wikipedia.org/wiki/Phytoplankton (accessed on 23 August 2023).
55. Keeling, R.F. The atmospheric oxygen cycle: The oxygen isotopes of atmospheric CO_2 and O_2 and the O_2/N_2 ratio. *Rev. Geophys.* **1995**, *33*, 1253–1262. [CrossRef]
56. Pries, C.H.; Angert, A.; Castanha, C.; Hilman, B.; Torn, M.S. Using respiration quotients to track changing sources of soil respiration seasonally and with experimental warming. *Biogeosciences* **2020**, *17*, 3045–3055. [CrossRef]
57. Robinson, C. Microbial Respiration, the Engine of Ocean Deoxygenation. *Front. Mar. Sci.* **2019**, *5*, 533. [CrossRef]
58. Tanioka, T.; Matsumoto, K. Stability of marine organic matter respiration stoichiometry. *Geophys. Res. Lett.* **2020**, *47*, e2019GL085564. [CrossRef]
59. Riser, S.C.; Johnson, K.S. Net production of oxygen in the subtropical ocean. *Nature* **2008**, *451*, 323–325. [CrossRef] [PubMed]
60. Ríos, A.f.; Fraga Pérez, F.F.; Figueiras, F.G. Chemical composition of phytoplankton and Particulate Organic Matter in the Ría de Vigo (NW Spain). *Sci. Mar.* **1998**, *62*, 257–271. [CrossRef]
61. Available online: https://oceanservice.noaa.gov/facts/exploration.html (accessed on 11 May 2023).
62. Available online: https://www.noaa.gov/education/resource-collections/ocean-coasts/ocean-acidification (accessed on 10 October 2023).
63. Mann, K.H.; Lazier, J.R.N. Chapter 10: The Oceans oand global Climate Change: Physcal and Bilofical Aspects. In *Dynamics of Marine Ecosystems: Biological-Physical Interactions in the Oceans*; Blackwell Scientific Publications: Boston, MA, USA, 1991; pp. 390–422.
64. Martin, M.S.; Vernet, M.; Cape, M.R.; Mesa, E.; Huertas, A.D.; Reigstad, M.; Wassmann, P.; Duarte, C.M. Relationship Between Carbon- and Oxygen-Based Primary Productivity in the Arctic Ocean, Svalbard Archipelago. *Front. Mar. Sci.* **2019**, *6*, 468. [CrossRef]
65. Annamalai, K. Oxygen Deficient (OD) Combustion and Metabolism: Allometric Laws of Organs and Kleiber's Law from OD Metabolism? *Systems* **2021**, *9*, 54. [CrossRef]
66. Popovic, M. Thermodynamic properties of microorganisms: Determination and analysis of enthalpy, entropy, and Gibbs free energy of biomass, cells and colonies of 32 microorganism species. *Heliyon* **2019**, *5*, 6. [CrossRef] [PubMed]
67. Kort, E.A.; Plant, G.; Brandt, A.R.; Chen, Y.; Fordice, G.; Negron AM, G.; Schwietzke, S.; Smith, M.; And Zavala-Araiza, D. Inefficient and unlit natural gas flares both emit large quantities of methane. *Science* **2022**, *377*, 1566–1571. [CrossRef]
68. Available online: https://chem.libretexts.org/Bookshelves/General_Chemistry/Book:_ChemPRIME_(Moore_et_al.)/03:_Using_Chemical_Equations_in_Calculations/3.03:_The_Limiting_Reagent/3.3.02:_Environment-_TSP_Ecological_Stoichiometry_and_Algal_Blooms (accessed on 28 October 2022).
69. Sosa Olivier, J.A.; Laines Canepa, J.R.; Guerrero Zarate, D.; González Díaz, A.; Figueiras Jaramillo, D.A.; Osorio García, H.K.; Evia López, B. Bioenergetic valorization of Sargassum fluitans in the Mexican Caribbean: The determination of the calorific value and washing mechanism. *Energy* **2022**, *10*, 45–63. [CrossRef]
70. Rosenberg, G.; Littler, D.S.; Littler, M.M.; Oliveira, E.C. Primary production and photosynthetic quotients of seaweeds from Sao Paulo State, Brazil. *Bot. Mar.* **1995**, *38*, 369–377. [CrossRef]
71. Available online: https://energy.appstate.edu/research/work-areas/cdiac-appstate (accessed on 20 August 2022).
72. Available online: https://data.ess-dive.lbl.gov/portals/CDIAC (accessed on 13 May 2023).
73. Available online: https://github.com/openclimatedata/global-carbon-budget/blob/main/archive/Global_Carbon_Budget_2019v1.0.xlsx (accessed on 2 May 2023).
74. Available online: https://www.ipcc.ch/report/land-use-land-use-change-and-forestry/ (accessed on 13 January 2022).
75. Available online: https://cdiac.ess-dive.lbl.gov/ftp/ndp030/global (accessed on 14 January 2023).
76. Fossil Fuels 'Stubbornly' Dominating Global Energy Despite Surge in Renewables: Energy Institute. Available online: https://www.spglobal.com/commodityinsights/en/market-insights/latest-news/oil/062623-fossil-fuels-stubbornly-dominating-global-energy-despite-surge-in-renewables-energy-institute (accessed on 16 November 2022).
77. Severinghaus, J.P. Studies of the Terrestrial O_2 and Carbon Cycles in Sand Dune Gases and in Biosphere 2. Ph.D. Thesis, Columbia University, New York, NY, USA, 1995.
78. Available online: https://ourworldindata.org/grapher/annual-change-fossil-fuels?tab=tabl (accessed on 10 August 2023).
79. Available online: https://ourworldindata.org/ (accessed on 18 October 2022).
80. Friedlingstein, P.; O'Sullivan, M.; Jones, M.W.; Andrew, R.M.; Hauck, J.; Olsen, A.; Peters, G.P.; Peters, W.; Pongratz, J.; Sitch, S.; et al. Global Carbon Budget 2020. *Earth Syst. Sci. Data* **2020**, *12*, 3269–3340. [CrossRef]
81. Keeling, R.F. Measuring correlations between atmospheric oxygen and carbondioxide mole fractions—A preliminary-study in urban air. *J. Atmos. Chem.* **1988**, *7*, 153–176. [CrossRef]

82. Annamalai, K.; Sweeten, J.M.; Ramalingam, S.C. Estimation of gross heating values of biomass fuels. *Trans. ASAE* **1987**, *30*, 1205–1208. [CrossRef]
83. Available online: https://ourworldindata.org/fossil-fuels#global-fossil-fuel-consumption (accessed on 24 August 2023).
84. Available online: https://scrippsco2.ucsd.edu/data/atmospheric_co2/primary_mlo_co2_record.html (accessed on 8 August 2023).
85. Ballantyne, A.P.; Alden, C.B.; Miller, J.B.; Tans, P.P.; White, J.W.C. Increase in observed net carbon dioxide uptake by land and oceans during the past 50 years. *Nature* **2012**, *488*, 70–72. [CrossRef] [PubMed]
86. Annamalai, K. Breathing Planet Earth: Global Respiratory Quotient (*RQ*glob) From Keeling's Data and CO_2-Budget among the Atmosphere, Land and Oceans. *J. Energies* 2023. *under review*.
87. Available online: https://www.osha.gov/laws-regs/standardinterpretations/2007-04-02-0 (accessed on 6 November 2023).
88. Keeling, R.F.; Powell, F.L.; Shaffer, G.; Robbins, P.A.; Simonson, T.S. Impacts of Changes in Atmospheric O_2 on Human Physiology. Is There a Basis for Concern? *Front. Physiol.* **2021**, *12*, 571137. [CrossRef]
89. Silva, M.; Lourenço, L.; Alves, R.D.F.B.; Sousa, L.F.; Almeida, S.E.D.S.; Farnese, F.S. Different ways to die in a changing world: Consequences of climate change for tree species performance and survival through an ecophysiological perspective. *Ecol. Evol.* **2019**, *9*, 11979–11999. [CrossRef]
90. Available online: https://www.ncei.noaa.gov/products/ocean-carbon-acidification-data-system (accessed on 1 November 2023).
91. Available online: https://www.epa.gov/climate-indicators/climate-change-indicators-ocean-acidity (accessed on 5 November 2023).
92. Available online: https://keelingcurve.ucsd.edu/2013/06/04/why-does-atmospheric-co2-peak-in-may (accessed on 13 October 2023).
93. Seo, K.-W.; Ryu, D.; Eom, J.; Jeon, T.; Kim, J.-S.; Youm, K.; Chen, J.; Wilson, C.R. Drift of Earth's Pole Confirms Groundwater Depletion as a Significant Contributor to Global Sea Level Rise 1993–2010. *Geophys. Res. Lett.* **2023**, *50*, e2023GL103509. [CrossRef]
94. Humans Are Pumping Out So Much Groundwater That It's Changing Earth's Tilt. Available online: https://www.space.com/earth-tilt-changed-by-groundwater-pumping (accessed on 8 November 2023).
95. Kumar, B. Consequences of Fossil Fuel Extraction on the Climate Change of the Earth. In Proceedings of the AGU Chapman Conference on Complexity and Extreme Events in Geosciences in India, Chapman Conference on Complexity and Extreme Events in Geosciences, National Geographical Research Institute, Hyderabd, India, 15–19 February 2010.
96. Ebeling, J.M.; Jenkins, B.M. Physical and chemical properties of biomass fuels. *Trans. ASAE* **1985**, *28*, 898–902. [CrossRef]
97. Popp, J.; Lakner, Z.; Harangi-Rákos, M.; Fari, M. The effect of bioenergy expansion: Food, energy, and environment. *Renew. Sustain. Energy Rev.* **2014**, *32*, 559–578. [CrossRef]